学位論文

Calcium regulation of microtubule sliding in reactivated flagella

運動中の鞭毛における微小管滑り運動の Ca^{2+} による制御機構

平成１１年　１２月博士（理学）申請
東京大学大学院理学系研究科
生物科学専攻
坂内　博子

学位論文

Calcium regulation of microtubule sliding in reactivated flagella

運動中の鞭毛における微小管滑り運動の Ca^{2+} による制御機構

平成１１年　１２月博士（理学）申請

東京大学大学院理学系研究科
生物科学専攻

坂内　博子

Contents

Summary

Oscillatory bending is a characteristic feature of the movement of eukaryotic flagella and cilia. The motive force for the oscillatory bending is active sliding induced by dynein arms among outer doublet microtubules in axonemes. The chemical energy, which is produced during hydrolysis of ATP by dynein ATPase activity, is converted to mechanical work, which induces sliding movement between outer doublet microtubules. The polarity of force generation induced by dynein is unidirectional. Thus, microtubule sliding between any two of the nine doublets should be regulated to generate oscillatory bending. Among the parameters of the microtubule sliding, the sliding pattern, and the sliding velocity have been investigated in previous studies, but the mechanism regulating the microtubule sliding within the axoneme has not been elucidated.

Ca^{2+} is one of the factors that modify the bending pattern of flagella and cilia. An increase in the intracellular Ca^{2+} concentration induces changes of the flagellar waveform. Changes in the pattern and velocity of microtubule sliding must underlie these waveform changes. In the previous studies, however, no significant effect of Ca^{2+} on microtubule sliding velocity has been demonstrated. Neither have axonemal components involved in the Ca^{2+} responses been identified. In this study, I have examined the effects of Ca^{2+} on the microtubule sliding in reactivated sea urchin sperm flagella to elucidate the mechanism by which Ca^{2+} regulates microtubule sliding in flagella. This is the first study in which the effect of Ca^{2+} on the microtubule sliding velocity in

beating flagella has been examined.

In Part 1, I aimed to detect the effects of Ca^{2+} on the microtubule sliding velocity of reactivated sperm flagella of sea urchin, *Hemicentrotus pulcherrimus*. I used the imposed head vibration technique to obtain stable flagellar beating. I analysed the bend angles of flagellar waves at vibration frequencies of 11-60 Hz and obtained the sliding velocity as the product of the bend angle and the beat frequency. I found that 10^{-6}-10^{-5} M Ca^{2+} decreased the maximum microtubule sliding velocity by about 15-20% at 27, 54 and 250 μM MgATP (about 50, 100 and 500 μM ATP). The Ca^{2+}-induced decrease of the sliding velocity was due mainly to a decrease in the reverse bend angle. When the plane of beat was artificially rotated by rotating the plane of vibration of the pipette that held the sperm head, the asymmetric bending pattern rotated at 10^{-5} M Ca^{2+} as well as at $<10^{-9}$ M Ca^{2+}. Such rotation of the beating plane at 10^{-5} M Ca^{2+} was observed in flagella reactivated at MgATP concentrations higher than 54 μM. These results indicate that the Ca^{2+}-induced decrease of sliding velocity is mediated by a rotatable component or components (probably the central pair) at high MgATP, but is not due to specific dynein arms on particular doublets. We further investigated the effects of a mild trypsin treatment and of calmodulin antagonists (trifluoperazine and W-7) on the Ca^{2+}-induced decrease in sliding velocity. In the axonemes treated for 3 minutes with a low concentration (0.1 μg/ml) of trypsin, neither Ca^{2+}-induced decrease in the microtubule sliding velocity nor that in the reverse bend angle

was observed. Trifluoperazine (25-50 μM) had no effect on the decrease of sliding velocity in beating flagella at 10^{-5} M Ca^{2+}. However, flagella that had been 'quiescent' at 10^{-4} M Ca^{2+} resumed asymmetrical beating following an application of 10-50 μM trifluoperazine. W-7 induced similar responses to those induced by trifluoperazine. Trypsin treatment induced a similar recovery of beating in quiescent flagella at 10^{-4} M Ca^{2+}, albeit with a more symmetrical waveform. These results indicate that mild trypsin-sensitive components may be associated with both the Ca^{2+}-induced decrease in sliding velocity and quiescence, but calmodulin may be associated only with quiescence.

In Part 2, I studied the effect of mild trypsin treatment on the axonemal proteins in order to gain some clues to the axonemal protein involved in the regulation of microtubule sliding in sea urchin sperm flagella. In Part 1, I demonstrated in the spermatozoa of *Hemicentrotus pulcherrimus* that the Ca^{2+}-induced decrease in the microtubule sliding velocity at 10^{-6} M Ca^{2+} was partially abolished by a 2 minute trypsin treatment and completely abolished by a 3 minute treatment and the induction of quiescence at 10^{-4} M Ca^{2+} was completely inhibited by a mild trypsin treatment longer than 2 minutes. Similar responses were also observed in the spermatozoa of the sea urchin *Anthocidaris crassispina*. I studied the axonemal components that were affected by a mild trypsin treatment by using SDS-polyacrylamide gel electrophoresis and found that at least twelve polypeptides were digested from the trypsin-treated axonemes in *Hemicentrotus* spermatozoa. Of the twelve,

eleven were digested by a 2-minutes trypsin treatment. The remaining (~160 kDa) polypeptide was digested only by a 3-minutes treatment. Thus, it seems possible that the ~160 kDa polypeptide is associated with the Ca^{2+}-induced decrease of sliding velocity. Calmodulin was digested by a 2-minutes trypsin treatment, which restored beating of quiescent flagella at 10^{-4} M Ca^{2+} in the spermatozoa of both sea urchins, *Hemicentrotus pulcherrimus* and *Anthocidaris crassispina*.

In the present study, I showed that the microtubule sliding velocity is regulated in a Ca^{2+} concentration dependent manner. This demonstrates for the first time that the effect of Ca^{2+} affects the microtubule sliding velocity. I also found that, at least at ATP concentrations higher than ~100 μM, the Ca^{2+}-induced decrease in sliding velocity in beating flagella is regulated through a trypsin-sensitive mechanism (~160 kDa polypeptide?) which possibly involves the central pair apparatus. An involvement of the central pair in the regulation of microtubule sliding in flagella and cilia has been controversial. The present study, however, showed that the central pair must play an important role in the regulation at higher MgATP concentrations, but that may not always be necessary for the regulation at lower MgATP conditions. I also found that calmodulin is not involved in the mechanism regulating the Ca^{2+}-induced decrease in sliding velocity, and that calmodulin may be associated with the mechanism underlying flagellar quiescence induced by 10^{-4} M Ca^{2+}.

General Introduction

1. Flagellar and ciliary motility

A characteristic feature of the movement of eukaryotic flagella and cilia is cyclical beating (or oscillatory bending). In flagella, bends are alternately initiated in opposite directions at the base and propagated towards the tip, while in cilia, bends are periodically initiated in one direction at the base and propagated towards the tip.

The cytoskeletal structure of flagella and cilia is called the axoneme. The axoneme is also called the '9+2' structure, because of its characteristic features observed by electron microscopy. It consists of nine sets of doublet microtubules in the periphery and two singlet microtubules in the centre (central pair). The doublet microtubules (or doublets) consist of two different microtubules, that is A-tubule of a complete tubule and B-tubule of an incomplete tubule. On the A-tubule there are two rows of dynein arms: the outer dynein arms and the inner dynein arms. The dynein arms on one A-tubule are projecting towards the B-tubule of adjacent doublet. Structures projecting from nine doublet microtubules towards the central pair are called the radial spokes. The heads of the radial spokes are closely located to the central sheath projections which are surrounding the central pair. Each two of the adjacent outer doublets are connected with the interdoublet links (or nexin links), as a result nine doublets are kept to be a circular tubule as a whole.

2. Function of the dynein arms

Dynein, the motor protein of eukaryotic flagella and cilia, was first reported by Gibbons (1963) and isolated by Gibbons and Rowe (1965) from *Tetrahymena* cilia as ATPase protein. Under an electron microscope, the isolated dynein arm appears as a bouquet, with two or three globular heads connected to a common base by a slender stem (Goodenough and Heuser, 1982). The globular heads contain ATPase sites as well as microtubule binding sites. There are two types of microtubule binding sites: the binding sites at the base of the dynein arm (binding to the A-tubule) and those in the head regions of the dynein arm (binding to the adjacent B-tubule) (Gee et al., 1997). *In vivo*, the base of the dynein arm is permanently attached to the microtubule (A-tubule). On the other hand, the tip of the dynein arm (so called B-link) is thought to undergo attachment-detachment cycles with the adjacent microtubules in an ATP-dependent manner, which forms the basis of microtubule sliding during the flagellar movement (Porter and Johnson, 1989; Omoto, 1991). Biochemical and electron microscopic studies suggest that this cycle, dynein cross-bridge cycle, consists of the following steps; (1) the dynein arm attached to the adjacent microtubule by its head in the absence of nucleotide (this state is called 'rigor') is released from the binding site on the microtubule when ATP binds to the dynein, (2) the dynein changes its conformation as the bound ATP is hydrolysed to ADP and Pi, (3) Pi dissociates from the dynein and the dynein reattaches to the new biding site on the microtubule, and, at the end of the

cycle, (4) the release of ADP triggers the power stroke. The rate-limiting step is the fourth step, the step of product release (Johnson, 1983; Omoto and Johnson, 1986; Porter and Johnson, 1989; Omoto, 1991). Conformational changes of dynein arms observed by electron microscope with quick-freeze deep-etch replica technique at different conditions of nucleotides support the above dynein cross-bridge cycles (Tsukita et al., 1983; Goodenough and Heuser, 1984; Sale et al., 1985). The power stroke (or mechanical work) generated by dynein arms provides force to slide their adjacent microtubules. The recent study by Tani and Kamimura (1999) suggested that the force generation begins at the dynein-ADP state after Pi is dissociated from the dynein at the third step. The polarity of force generation by dynein arms is unidirectional (Sale and Satir, 1977; Fox and Sale, 1987): active dynein moves the adjacent microtubules from base (the minus end of the microtubule) to tip in flagella (the plus end of the microtubule), as a result microtubules from which the active dynein arms are projected move against their adjacent microtubules toward the base in flagella.

3. Regulation of active sliding during flagellar beating

The motive force for the cyclical bending of flagella and cilia is based on active sliding among doublet microtubules induced by cyclical activity of dynein arms. The first direct evidence of the active microtubule sliding in the axoneme was shown by Summers and Gibbons (1971): mild digestion of axonemes by trypsin

could induce active sliding movement of doublet microtubules in the presence of MgATP. In 1988, Vale and Toyoshima showed that isolated dyneins, which are absorbed onto a glass surface, could induce gliding movement of microtubules on the glass by *in vitro* motility assay experiments. Direct measurements of microtubule sliding in demembranated and reactivated sperm flagella have been done by Brokaw (1989) who used gold microbeads attached on the doublets as markers of positions on the doublets. An experiment of local reactivation of the axoneme done by Shingyoji et al. (1977) strongly demonstrated that the flagellar bending is the result of microtubule sliding.

Sliding between microtubules can be converted to bending movement of the flagellum only if the sliding is regulated in the axoneme. The polarity of force generation by the dynein arms is from base to tip in flagella. Thus, if the same active sliding occurred at nine interdoublet sites simultaneously, the axoneme would only twist without generating a planar bend characteristic of flagellar movement. To generate a planar bend, the following two mechanisms are required: firstly, sliding among doublets should be regulated to produce a bend. More precisely, sliding should be regulated so that the maximal sliding displacement occurs in the interdoublet sites on or near the plane, which is perpendicular to the beat plane and is usually in the same plane with the central pair microtubules (Takahashi et al., 1982). Secondly, when a bend is generated in one direction, a half of the nine doublets should actively slide

while the other half are passively displaced. Otherwise, the pair of forces generated in the counteracting interdoublet sites simultaneously would act antagonistically to prevent bending (Brokaw and Gibbons, 1975). When a new bend is generated in the opposite direction, those doublets that had slid passively during the previous bending should now slide actively. These processes of alternate activation and inactivation of force generation (or generation of sliding) have hypothesized as 'switching' of dynein activity (Satir and Sale, 1977; Wais-Steider and Satir, 1979; Tamm and Tamm, 1981, 1984; Satir, 1982, 1985). Regulation of these mechanisms has been unclear, although the regulation of dynein activity necessary for the maximal sliding displacement in the axoneme is thought to be closely related to the central pair (this will be discussed in Part 1).

4. Ca^{2+} regulation of flagellar and ciliary motility

An important aspect of flagellar and ciliary motility is that, in addition to the basic regulatory mechanism of microtubule sliding, the movement of these organelles themselves is controlled. In many organisms, external stimuli modify some parameters, such as beat frequency and beat direction in the movement of flagella and cilia. When a *Paramecium* collides against an obstacle, the direction of effective stroke in ciliary beating changes, as a result the organism can change its swimming direction to avoid the obstacle. *Chlamydomonas* with asymmetrical (ciliary type) beating flagella swims

forward and it changes to swim backward when bright flash light induces symmetrical (flagellar type) beating flagella (Rüffer and Nultsh, 1991; Schmidt and Eckert, 1976). In these responses, intracellular Ca^{2+} has been shown to play an important role.

To examine effects of Ca^{2+} on flagellar and ciliary motility, Ca^{2+} must be applied to the axoneme directly. When the membrane is removed from cilia or flagella, the endogenous ATP is lost and the movement ceases. The addition of exogenous ATP causes the demembranated flagella or cilia to resume beating. This process is called reactivation. Various effects of Ca^{2+} on flagellar and ciliary movement have been reported by using reactivated flagella and cilia. Thus, a high concentration of Ca^{2+} (above 10^{-6}-10^{-5} M), reverses the direction of beat in the demembranated *Paramecium* (Naitoh and Kaneko, 1972). It also alters the symmetry of the flagellar waveform in the demembranated *Chlamydomonas* (Hyams and Borisy, 1978; Bessen et al., 1980). In the sea urchin sperm flagella, Ca^{2+} (10^{-6}-10^{-5} M) increases the asymmetry of bending waves and, at higher concentrations (10^{-4} M) arrests the beating (see below). These changes in waveforms are thought to be caused by regulation of sliding activity of dynein, but the molecular basis of the effect of Ca^{2+} on sliding activity in flagella and cilia is poorly understood. There are some reports to suggest the roles of the central pair in the regulation of sliding, but this is still controversial.

5. Ca^{2+} regulation of flagellar motility in sea urchin sperm

Sea urchin sperm flagella have been used for the physiological, biochemical, and biophysical studies on the mechanism of flagellar motility. Their relatively large size, 40-50 μm in length, is an advantage for the analysis of bending wave parameters. The waveform of sea urchin sperm flagella consists of a principal bend with a larger bend angle and a reverse bend with a smaller bend angle (Gibbons and Gibbons, 1972). These bends are formed alternately on opposite sides of the head axis and in a single beat plane.

As in other flagella and cilia, Ca^{2+} plays important roles in the regulation of flagellar motility of sea urchin sperm. Ca^{2+} modifies the symmetry of the waveform: a higher concentration of Ca^{2+} increases the angle of principal bends and decreases the angle of reverse bends so that the degree of asymmetry of waveform (differences between the bend angles of principal and reverse bends) is amplified (Brokaw, 1979). At a much higher concentration of Ca^{2+}, flagella become quiescent in a characteristic cane shaped form (Gibbons and Gibbons, 1980). Similar changes in waveform can be observed in swimming live spermatozoa. Spermatozoa change the symmetry of bending waves when they collide against some obstacle, such as a glass microneedle and transiently stop swimming in a quiescent form when a blue light or an electrical stimulation is applied (Gibbons, 1980; Shingyoji and Takahashi, 1995a). Therefore, these Ca^{2+} responses must be essential for the modification of swimming direction in sea urchin spermatozoa. As in other flagella and cilia,

the mechanism of the Ca^{2+} responses in sea urchin sperm flagella has not been clear. In particular, the mechanism that controls active sliding in a Ca^{2+}-dependent manner is poorly understood.

6. Plan of the thesis

The aim of this study has been to examine the effect of Ca^{2+} on the sliding activity of dynein and to identify the structural element involved in the Ca^{2+} responses in sea urchin spermatozoa. In Part 1, I have investigated the effect of Ca^{2+} on the microtubule sliding velocity by analysing the waveform of reactivated sperm. In the previous studies, in which axonemes treated with proteases or isolated dynein arms were used, no effect of Ca^{2+} on the microtubule sliding velocity was detected. I thought that the regulatory system, which is probably affected by proteolysis or isolation of dynein, must play important roles to regulate the sliding activity of dynein. Therefore intact reactivated flagella have been used in this study. By employing imposed head vibration technique and waveform analysis, I measured the apparent microtubule sliding velocity in beating flagella at various Ca^{2+} conditions. I found that 10^{-6}-10^{-5} M Ca^{2+} reduced the sliding velocity at 27-250 μM MgATP accompanied by a decrease in reverse bend angle. This Ca^{2+}-induced decrease in sliding velocity was closely associated with the rotation of the beating plane at ATP concentration higher than 100 μM. These results clearly show that Ca^{2+} reduces the sliding velocity in beating flagella and this is mediated by a

regulatory signal from a rotatable components, probably the central pair. The results in this study provide the answer to the contradictions concerning the roles of the central pair at various Ca^{2+} conditions.

In order to understand the molecular basis of the Ca^{2+}-responses, I also examined the effects of mild trypsin treatment and calmodulin antagonists on the Ca^{2+}-induced decrease in sliding velocity and on the formation of quiescence. Mild trypsin treatment is reported to remove some Ca^{2+}-dependent responses (Brokaw and Simonick, 1977; Gibbons and Gibbons, 1980). In this study it abolished the Ca^{2+}-induced decrease in sliding velocity as well as the induction of quiescence. Calmodulin is present in sea urchin sperm flagella (Burgess et al., 1980; Brokaw and Nagayama, 1985) but its role has been unclear. In this study, calmodulin antagonists did not affect the sliding velocity but inhibited the induction of quiescence. These results suggest that the mild trypsin-sensitive components may be involved in the Ca^{2+}-induced decrease in sliding velocity while calmodulin may be associated with the mechanism underlying flagellar quiescence induced by 10^{-4} M Ca^{2+}.

In Part 2, I tried to study proteins involved in the Ca^{2+}-induced decrease in sliding velocity and the quiescence. Based on the results concerning the effects of mild trypsin treatment and calmodulin antagonists in Part 1, I investigated the effects of mild trypsin treatment on polypeptides of the axoneme by SDS-PAGE. Although the data were still preliminary, twelve polypeptides including calmodulin were affected by mild trypsin treatment. Some of the twelve may

be associated with the Ca^{2+}-induced decrease in sliding velocity.

Part 1

Effects of Ca^{2+} on microtubule sliding velocity and sliding pattern in reactivated sea urchin sperm flagella

SUMMARY

The changes in the bending pattern of flagella induced by an increased intracellular Ca^{2+} concentration are caused by changes in the pattern and velocity of microtubule sliding. However, the mechanism by which Ca^{2+} regulates microtubule sliding in flagella has been unclear. To elucidate it, I studied the effects of Ca^{2+} on microtubule sliding in reactivated sea urchin sperm flagella that were beating under imposed head vibration. I found that the maximum microtubule sliding velocity obtainable by imposed vibration, which was about 170-180 rad/second in the presence of 250 μM MgATP and $<10^{-9}$ M Ca^{2+}, was decreased by 10^{-6}-10^{-5} M Ca^{2+} by about 15-20%. Similar decrease of the sliding velocity was observed at 54 and 27 μM MgATP. The Ca^{2+}-induced decrease of the sliding velocity was due mainly to a decrease in the reverse bend angle. When the plane of beat was artificially rotated by rotating the plane of vibration of the pipette that held the sperm head, the asymmetric bending pattern also rotated at 10^{-5} M Ca^{2+} as well as at $<10^{-9}$ M Ca^{2+}. The rotation of the bending pattern was observed at MgATP higher than 54 μM (~100 μM ATP). These results indicate that the Ca^{2+}-induced decrease of the sliding velocity is mediated by a rotatable component or components (probably the central pair) at high MgATP, but is not due to specific dynein arms on particular doublets. I further investigated the effects of a mild trypsin treatment and of trifluoperazine on the Ca^{2+}-induced decrease in sliding velocity. Axonemes treated for 3 minutes with a low concentration (0.1 μg/ml)

of trypsin beat with a more symmetrical waveform than before the treatment. Also, their microtubule sliding velocity and reverse bend angle were not affected by high Ca^{2+} concentrations. Trifluoperazine (25-50 μM) had no effect on the decrease of the sliding velocity in beating flagella at 10^{-5} M Ca^{2+}. However, the flagella that had been 'quiescent' at 10^{-4} M Ca^{2+} resumed asymmetrical beating following an application of 10-50 μM trifluoperazine. In such beating flagella, both the sliding velocity and the reverse bend angle were close to their respective values at 10^{-5} M Ca^{2+}. Trypsin treatment induced a similar recovery of beating in quiescent flagella at 10^{-4} M Ca^{2+}, albeit with a more symmetrical waveform. These results provide first evidence that, at least at ATP concentrations higher than ~100 μM, 10^{-6}-10^{-5} M Ca^{2+} decreases the maximum sliding velocity of microtubules in beating flagella through a trypsin-sensitive regulatory mechanism which possibly involves the central pair apparatus. They also suggest that calmodulin may be associated with the mechanism underlying flagellar quiescence induced by 10^{-4} M Ca^{2+}.

INTRODUCTION

Flagellar and ciliary bending patterns are known to change in response to an increase in the intracellular Ca^{2+} concentration (Naitoh and Kaneko, 1972; Holwill and McGregor, 1976; Hyams and Borisy, 1978). In sea urchin sperm flagella, 10^{-6}-10^{-5} M Ca^{2+} increases the asymmetry of waveform and a higher concentration of Ca^{2+} (~10^{-4} M) induces a stoppage of flagellar beating ('quiescence') characterized by a large cane-shaped bend in the proximal region (Brokaw, 1979; Gibbons and Gibbons, 1980). These changes of waveform are thought to be caused by changes in the sliding activity of microtubules within the axoneme. The effect of Ca^{2+} on microtubule sliding has not been definitively demonstrated nor have the axonemal components involved in the Ca^{2+} response been identified. In previous studies, the sliding velocity was measured either by analysing the movement of doublet microtubules in axonemes that were undergoing disintegration as the result of trypsin treatment (Yano and Miki-Noumura, 1980; Takahashi et al., 1982; Okagaki and Kamiya, 1986) or by analysing the gliding movement of microtubules on isolated dynein (Sale and Fox, 1988; Vale and Toyoshima, 1989; Kagami and Kamiya, 1992; Sakakibara and Nakayama, 1998). In either case, the sliding velocity was unaffected by the Ca^{2+} concentration (Walter and Satir, 1979; Mogami and Takahashi, 1983; Okagaki and Kamiya, 1986; Vale and Toyoshima, 1989). This may indicate that if Ca^{2+} affects the microtubule sliding, it does not regulate all the dynein arms

uniformly. If this is the case, specific dynein arms on particular doublets and/or a regulatory component or components, such as the central pair and the radial spokes, may be involved in the Ca^{2+}-regulation of the dynein activity. In the previous two approaches, the activity of some specific dynein arms may not have been distinguished from that of the other dynein arms. Furthermore, these procedures seem to have precluded the detection of possible function of the regulatory components.

In order to overcome the difficulties in the previous approaches and detect the effect of Ca^{2+} on the sliding activity, I employed the imposed head vibration method. Live or reactivated sea urchin spermatozoa held by their heads in the tip of a vibrating micropipette can be forced to synchronize their flagellar beat with the imposed vibration (Gibbons et al. 1987; Shingyoji et al., 1991a, 1995). In this way, both the beat frequency and the beat plane could be modulated without loss of either stability or regularity of the waveform. This technique enabled us to analyse stably beating flagella at various beat frequencies and calculate the microtubule sliding velocity as the product of the beat frequency and the bend angle. In the present study, I was able to impose head vibration on reactivated flagella at 10^{-6}-10^{-5} M Ca^{2+} to induce stable beating and to detect a Ca^{2+}-induced decrease in the microtubule sliding velocity in the presence of functional regulatory components.

To determine whether specific dynein arms or regulatory components are involved in the mechanism regulating the Ca^{2+}-induced decrease of the sliding velocity, I used the method of artificial rotation of the flagellar beat plane. In a similar arrangement as above, rotation of the plane of pipette vibration around the head axis induces corresponding rotation of the plane of beating. The imposed rotation of the waveform is the result of rotation of the coordinated pattern of sliding among the doublet microtubules of the axoneme (Shingyoji et al., 1991b). In this study, I found that the beat plane rotated with the rotation of the vibration plane even at high Ca^{2+} concentrations where the characteristic asymmetry of waveform accompanied the rotating plane of beat.

I further examined the effects of mild trypsin treatment and calmodulin antagonists on the Ca^{2+}-induced decrease in sliding velocity at 10^{-6}-10^{-5} M Ca^{2+} and on the quiescence induced by 10^{-4} M Ca^{2+}. Mild trypsin treatment is known to remove some Ca^{2+}-dependent responses, such as an increased asymmetry and the quiescence (Brokaw and Simonick, 1977; Gibbons and Gibbons, 1980). I studied its effect on the Ca^{2+}-induced decrease in sliding velocity. Calmodulin is present in sea urchin sperm flagella (Burgess et al., 1980; Brokaw and Nagayama, 1985) but its role has been unclear. I used calmodulin antagonists trifluoperazine and W-7 to identify the role, if any, of calmodulin in the regulation of the sliding velocity and the sliding pattern of microtubules.

MATERIALS AND METHODS

Reactivation of spermatozoa

Spermatozoa of the sea urchin, *Hemicentrotus pulcherrimus*, were suspended in 2,000 volumes of Ca^{2+}-free artificial sea water containing 465 mM NaCl, 10 mM KCl, 25 mM $MgSO_4$, 0.2 mM ethylenediaminetetraacetic acid (EDTA) and 2 mM Tris-HCl (pH 8.2). The suspended spermatozoa were demembranated with 40 volumes of demembranating solution under the 'potentially asymmetric' conditions (Gibbons and Gibbons, 1980) and reactivated with the reactivating solution. The demembranating solution contained 0.04% (w/v) CHAPS (3-[(3-cholamidopropyl) dimethylammonio]-1-propane-sulphonate), 0.01% (w/v) Nonidet P-40, 0.2 M potassium acetate, 2 mM $MgSO_4$, 2 mM glycoletherdiamine-*N, N, N', N'*-tetraacetic acid (EGTA), 20 mM Tris-HCl (pH 8.2), and 1 mM dithiothreitol (DTT) and the reactivating solution contained 0.2 M potassium acetate, 2 mM $MgSO_4$, 2 mM EGTA, 20 mM Tris-HCl (pH 8.2), 2% (w/v) polyethylene glycol (PEG; *Mr* 20×10^3), 1 mM DTT and various concentrations of ATP with or without $CaCl_2$ (Katada et al., 1989). The amounts of ATP and $CaCl_2$ added to the reactivating solution were calculated so as to obtain constant concentrations of MgATP (250, 54 and 27 μM) at $<10^{-9}$, 10^{-6}, 10^{-5} and 10^{-4} M Ca^{2+}. MgATP concentrations of 250, 54 and 27 μM at $<10^{-9}$ M Ca^{2+} correspond to ATP concentrations of 500, 100 and 50 μM, respectively. All experiments were carried out at room temperature (24-26°C).

Mild trypsin treatment and treatment with TFP

For trypsin treatment, I slightly modified the method developed by Brokaw and Simonick (1977). Spermatozoa of sea urchin *Hemicentrotus pulcherrimus* and *Anthocidaris crassispina* were suspended in about 20 volumes of Ca^{2+}-free artificial sea water to give an optical density reading of 0.2 when the suspended spermatozoa were further diluted with 1:100 with artificial sea water. The suspended spermatozoa were then demembranated with 6 volumes of demembranating solution. After 45 seconds, the demembranated sperm suspension was added to 11 volumes of reactivating solution without PEG and ATP and containing 0.1 μg/ml trypsin. Digestion was carried out for 2 or 3 minutes at 27.0±0.1°C and stopped with an addition of an excess volume of soybean trypsin inhibitor (0.25 μg/ml for motility). For motility observation, 2 μl of trypsin-treated spermatozoa were reactivated in 1 ml reactivating solution (with PEG) containing 250 μM MgATP with or without 10^{-6}-10^{-4} M Ca^{2+}.

For TFP treatment, TFP (final concentration: 10-50 μM) was added to the reactivating solution at 250 μM MgATP with or without 10^{-5}-10^{-4} M Ca^{2+}. After 2-15 minutes incubation, vibration was applied to the beating sperm held by the micropipette (see below) and their waveform was analysed.

Reagents

ATP was purchased from Boehringer Mannheim, trypsin (Type III) and soybean trypsin inhibitor (Type I-S) from SIGMA, trifluoperazine (TFP)

dimaleate from Wako (Osaka, Japan). N-(6-aminohexyl)-5-chloro-1-naphtolene sulfonamide (W-7) hydrochloride was from TOCRIS (MO, USA).

Observation and recording

Flagellar movement was observed under an inverted microscope with phase-contrast optics (Zeiss Axiovert 35). The movements of the flagellum and a micropipette were recorded on video tape at 200 frames/second with a high-speed video system (nac MHS200), using xenon flash illumination synchronized to the recording frequency (Shingyoji et al., 1991b).

Vibration of micropipette and rotation of the vibration plane

The methods for holding a sperm head with a micropipette, vibration of the micropipette, and rotation of the plane of vibration were the same as used in the previous studies (Shingyoji et al., 1991a, b). Spermatozoa were vibrated at frequencies of 15-60 Hz with amplitudes (peak-to-peak) of 17-26 μm by applying in-phase sinusoidal voltages generated by computer programme to two orthogonal piezoelectric bimorphs (Fig. 1-1) (Gibbons et al., 1987; Shingyoji et al., 1995). Rotation of the vibration plane was performed at about 0.2 revolution per second, and the directions of the rotation were counterclockwise (for definition, see Shingyoji et al., 1991b).

Waveform analysis and calculation of microtubule sliding velocity

The method I used for waveform analysis was the same as described previously (Shingyoji et al., 1995). Flagellar images were traced from the monitor screen, digitized and stored as values of angular orientation relative

to the axis of the sperm head. I obtained the angles of principal bends and reverse bends by differentiating the shear angle curves (Shingyoji et al., 1995). I analysed 28-32 images of flagella under each set of frequency and experimental conditions for each spermatozoon. I calculated the microtubule sliding velocity at a given point on the flagellum as the product 2 × (beat frequency) × (averaged angle of principal and reverse bends centered at the point in question) (Shingyoji et al., 1991a, 1995; Brokaw, 1991b). This product is proportional to the time averaged velocity of sliding between doublet microtubules. For statistical analysis, I obtained the average sliding velocities from 6-7 sperm (i.e. 180-210 images).

The highest sliding velocities are always observed in the proximal region, which may be the result of passive sliding or elastic distortion of the microtubule due to the direct effect of vibration (Eshel and Gibbons, 1989; Shingyoji et al., 1991a, 1995). In contrast, the sliding velocities in the middle region of the flagella are not directly affected by the head vibration. In the more distal regions, the sliding velocities attenuate due to a bend attenuation. Thus I took the bend angles at 5-17 μm (5-10 μm for TFP experiments) from the base of the flagella where the highest bend angles were observed to calculate the sliding velocity in the proximal region, and bend angles at 20-25 μm (15-25 μm for TFP experiments) from the base where the direct effects of head vibration and bend attenuation were not observed to calculate the sliding velocity in the middle region (Fig. 1-1). In

the case of trypsin treatment, the largest bend angles were observed at 3-8 μm from the base and the bend attenuation started at about 20 μm from the base, so I chose 10-20 μm from the base as the middle region.

RESULTS

Effect of Ca^{2+} on the sliding velocity under imposed head vibration

In the solution containing 250 μM MgATP and 10^{-5} M Ca^{2+}, flagellar axonemes beat at 35.4±2.7 Hz (n=22), which was similar to the frequency at $<10^{-9}$ M Ca^{2+} ('natural' beat frequency, 35.6±3.2 Hz; n=34). When the spermatozoa were held by their head with a micropipette and vibrated laterally (parallel to the surface of the slide glass) at a frequency close to the natural beat frequency, the flagella showed stable beating in synchrony with the imposed movement (Shingyoji et al., 1991a, 1995). Increasing and decreasing the vibration frequency within a range of about 20-60 Hz was immediately followed by synchronized stable beating at the new frequency. Fig. 1-2 shows typical tracings of the spermatozoa during vibration at 26 Hz, 35 Hz, and 45 Hz and at $<10^{-9}$ M (upper tracings) and 10^{-5} M Ca^{2+} (lower tracings).

Fig. 1-3 summarizes the average sliding velocities at various vibration frequencies, each of which was calculated from the bend angle and the beat frequency, in the proximal region and the middle region of the flagella. In the proximal region (Fig. 1-3A), the sliding velocity increased as the vibration

frequency increased from 20 to 60 Hz. This increase in the proximal region may be due to a large contribution of a passive sliding between the microtubules or an elastic distortion of the microtubules due to the imposed vibration in addition to the active microtubule sliding. The sliding velocity in the proximal region at 10^{-5} M Ca^{2+} was not significantly different from that at $<10^{-9}$ M Ca^{2+} at any vibration frequency between 20 and 60 Hz.

In the middle region (Fig. 1-3B), the sliding velocity decreased as the vibration frequency decreased below the natural beat frequency, but plateaued as the vibration frequency was increased over the natural beat frequency. Similar effects were observed at both $<10^{-9}$ M and 10^{-5} M Ca^{2+}. In the middle region, contribution of passive microtubule sliding or elastic distortion to the sliding velocity would be much smaller than in the proximal region and the sliding velocity is thought to be caused mainly by active sliding between the microtubules. The determinant of this 'maximum' sliding velocity obtainable by imposed vibration at or above the natural beat frequency is the MgATP concentration (Shingyoji et al., 1995). Although Ca^{2+} did not affect the profile of the sliding velocity changes, the sliding velocities at 10^{-5} M Ca^{2+} were lower than those at $<10^{-9}$ M Ca^{2+} at most vibration frequencies. At the vibration frequency of 35 Hz (near the natural beat frequency) and 45 Hz (higher than the natural beat frequency), the sliding velocity at 10^{-5} M Ca^{2+} (about 140 rad/second) was significantly smaller than that at $<10^{-9}$ M Ca^{2+} (about 170 rad/second) ($p<0.01$ and $p<0.02$, t-test),

while the sliding velocity at 21 Hz (lower than the natural beat frequency) (about 115 rad/second) did not differ significantly between the two Ca^{2+} concentrations ($p>0.2$, t-test) (Fig. 1-4A). These differences in the sliding velocity caused by Ca^{2+} at 35 and 45 Hz were due to a significant decrease in the bend angle of the reverse bend ($p<0.001$ at 35 Hz, and $p<0.02$ at 45 Hz) (Fig. 1-4B) while the bend angle of the principal bend did not change by the presence or absence of Ca^{2+} (Fig. 1-4C).

I obtained a similar decrease of the maximum sliding velocity by Ca^{2+} at lower MgATP concentrations (54 and 27 μM) (Fig 5A). At a vibration frequency near the natural beat frequency, the maximum average sliding velocity at $<10^{-9}$ M Ca^{2+} (92.3±15.1 rad/second, n=5, at 54 μM and 57.9±8.6 rad/second, n=5, at 27 μM) significantly decreased by about 20% at 10^{-5} M Ca^{2+} (73.7±8.2 rad/second at 54 μM, 45.3±5.9 rad/second at 27 μM). This decrease in the sliding velocity was also due to a decrease in the reverse bend angle (Fig. 1-5B, C).

Effect of Ca^{2+} on rotation of the beat plane

I was interested in whether Ca^{2+} acts directly on specific dynein arms on particular peripheral doublets, or it acts on some other mechanism that controls the reverse bend formation. To answer this question, I examined whether the decrease in the reverse bend angle was associated with particular doublet microtubules when the beat plane was rotated. In sea

urchin sperm flagella, the rotation of the plane of pipette vibration around the head axis induces corresponding rotation of the plane of beating and the orientation of principal bend and reverse bend counterchanges after the rotation of 180 degrees (Gibbons et al., 1987; Katada et al., 1989; for video images of the rotation of the beat plane, see Omoto et al., 1999) (Fig. 1-6A). It has been shown that the peripheral doublet microtubules do not rotate when the beat plane rotates by observing microbeads attached on the doublets (Fig. 1-6B) (Shingyoji, et al., 1991b). The imposed rotation of the waveform is thus the result of rotation of the coordinated pattern of sliding among the doublet microtubules of the axoneme, and is not accompanied by a twisting of the whole axonemal structure. If Ca^{2+} affects specific dynein arms on particular doublets and decreases the reverse bend angle, then the principal bend angle will decrease and the reverse bend angle will increase after a 180-degree rotation of the beat plane. On the other hand, if Ca^{2+} acts on the mechanism regulating the pattern of sliding that determines the side on which the reverse bend is formed, the principal and reverse bends will counterchange with the 180-degree rotation of the beating plane since the regulating mechanism rotates. Fig. 1-7A shows typical tracings of flagella before (left tracings) and after (right tracings) a 180-degree rotation of the beat plane, while being vibrated at 35 Hz (at 250 μM MgATP). Both in the absence (upper panels) and the presence (lower panels) of Ca^{2+}, the flagellar asymmetry rotated 180 degrees with the 180-degree rotation of the plane of

micropipette vibration. This is also seen clearly in the average bend angles of the principal bends and the reverse bends in the middle region of the flagellum before and after the rotation of the beat plane (Fig. 1-7B). The principal bend angles were not changed by the rotation of the beating plane at $<10^{-9}$ M as well as at 10^{-5} M Ca^{2+} ($p>0.3$, t-test). The bend angles of the reverse bend also did not change with the rotation of the beat plane ($p>0.3$, t-test). However, they decreased significantly at 10^{-5} M Ca^{2+} compared with those at $<10^{-9}$ M Ca^{2+} both before and after the rotation. These results support the counterchanges of the principal and the reverse bends with the rotation of the beat plane. Similar rotation of the bending pattern at both $<10^{-9}$ M and 10^{-5} M Ca^{2+} was observed at 54 μM as well as 250 μM MgATP. At 27 μM MgATP, however, rotation of the beat plane could not be observed as spontaneous 'unwinding' (Takahashi et al., 1991) took place when the rotation of the plane of vibration exceeded 90 degrees. I conclude that Ca^{2+} does not act directly on specific dynein molecules on particular peripheral doublets, but, at least at high MgATP concentrations, acts on some mechanism that controls the bend formation and the sliding pattern.

Effects of mild trypsin treatment on the Ca^{2+}-induced decrease of sliding velocity

I examined the effects of mild trypsin (0.1 μg/ml) treatment on the sliding velocity and on the reverse bend angle in flagella beating at 35 Hz under

imposed vibration. Before starting the vibration, the axonemes that had been treated with trypsin for 2 minutes beat with more symmetrical waveforms than they did before the treatment. After a 3 minutes-treatment, symmetrical flagellar beating was observed in most of the axonemes except a very few axonemes that showed sliding disintegration without beating. The proportion of the axonemes showing sliding disintegration increased gradually with an increase of the duration of trypsin treatment. Imposition of vibration brought about synchronization of the flagellar waves in the trypsin treated axonemes to the pipette vibration, as in the untreated axonemes (Fig. 1-8). Before the trypsin treatment, the sliding velocity at 10^{-6} M Ca^{2+} was smaller than that at $<10^{-9}$ M Ca^{2+} by about 15% (Fig. 1-9A, asterisk). This Ca^{2+}-dependent decrease in the sliding velocity was abolished by the trypsin treatment of both 2 and 3 minutes (Fig 1-9A). In the 2 minutes-treated axonemes, however, the bend angle of the reverse bend was still significantly smaller at 10^{-6} M Ca^{2+} than that at $<10^{-9}$ M Ca^{2+}, while such a difference was not observed in the 3 minutes-treated axonemes (Figs. 1-8 and 1-9B). The principal bend angles were not significantly affected by the 3-minutes trypsin treatment at both $<10^{-9}$ M and 10^{-6} M Ca^{2+} (Fig. 1-9C).

Effects of TFP on the Ca^{2+}-induced decrease in sliding velocity

As shown in Table 1, TFP did not change the sliding velocity at $<10^{-9}$ M Ca^{2+}. Also, the significant decrease of the sliding velocity was observed at 10^{-5} M Ca^{2+} regardless of the presence of 25-50 μM TFP. The significant decrease of the reverse bend angle due to an increase of Ca^{2+} was also observed in the TFP-treated as well as in the untreated axonemes. These results indicate that TFP does not inhibit the Ca^{2+}-induced decrease of the sliding velocity and the role of calmodulin at 10^{-5} M Ca^{2+} may be small, if any.

Recovery of beating of 'quiescent' flagella

TFP showed a significant effect at a higher Ca^{2+} concentration. At 10^{-4} M Ca^{2+}, it restored stable asymmetrical beating of 'quiescent' flagella (Fig. 1-10, upper tracings). The recovery of beating was induced in 100% of the quiescent flagella immediately after the application of 10-50 μM TFP. The average sliding velocity in the middle region of the flagella that had resumed beating upon application of 10 μM TFP was 138 rad/second under imposed head vibration (Table 1). This was close to the sliding velocity at 10^{-5} M Ca^{2+}. The reverse bend angle also restored the 10^{-5} M Ca^{2+} level. Similar resumption of beating was observed when I used W-7 (20 μM) instead of TFP. Thus, I conclude that calmodulin is involved in the mechanism regulating the 'quiescence'.

I also found that mild trypsin treatment longer than 2 minutes restored beating in 'quiescent' flagella at 10^{-4} M Ca^{2+} but with a more symmetrical

waveform than that of the TFP-treated flagella (Fig. 1-10, lower tracings).

DISCUSSION

The present study has shown that the velocity of microtubule sliding in flagella that were beating under imposed head vibration was decreased by Ca^{2+}. This is the first quantitative analysis to show the effect of Ca^{2+} on the microtubule sliding velocity. The head vibration technique (Gibbons et al., 1987; Shingyoji et al., 1991a, 1995) allowed us to calculate the apparent sliding velocity of microtubules in the beating flagella. I found that Ca^{2+} significantly decreased the maximum sliding velocity in the middle region of the flagella. Since the decrease of the sliding velocity was observed over a wide range of MgATP concentrations (27-250 μM), the absolute value of the sliding velocity and the absolute concentration of the MgATP are not essential factors for the regulation by Ca^{2+}. Thus, I conclude that the maximum sliding velocity, which represents active sliding between doublet microtubules at a given MgATP concentration and which depends directly on the concentration of MgATP, is regulated by Ca^{2+}.

Calcium-induced changes in the microtubule sliding velocity have not been detected in the previous studies, in which either the sliding disintegration of axonemes treated with trypsin (~1 μg/ml) (Walter and Satir, 1979; Mogami and Takahashi, 1983; Okagaki and Kamiya, 1986), or gliding of microtubules on isolated axonemal dynein were analysed (Vale

and Toyoshima, 1989). The trypsin-treated axonemes and the isolated dynein have lost the mechanism regulating the sliding activity to induce bending movement (Shingyoji and Takahashi, 1995b). The present results clearly demonstrate that the mechanism that is lost in both the trypsin-treated axonemes and the isolated dynein is essential for the Ca^{2+} regulation of the sliding activity of dynein. Furthermore, this mechanism is closely associated with the regulation of sliding necessary for the reverse bend formation. In the previous studies, the bend formation has been thought to be closely related to the sliding activity of specific dynein arms on particular doublets. Thus, Sale (1986) suggested that sliding between doublets 7 and 8 is responsible for the generation of the principal bends while that between doublets 3 and 4 is responsible for the formation of the reverse bends, and the sliding between doublets 3 and 4 may be specifically inhibited by Ca^{2+}. However, our present results indicate that the reverse bend is not always formed by the sliding between the specific doublets such as 3 and 4. Therefore Ca^{2+} does not always inhibit the microtubule sliding between the doublets 3 and 4, but inhibits sliding between any adjacent doublets involved in the formation of the reverse bends. It is likely that the regulatory mechanism is associated with the axonemal components that is capable of rotation.

What then are the rotatable structural components that are involved in the regulation of the microtubule sliding? The central pair apparatus is the

only structural component known to be capable of rotation within the axoneme. The rotation of the central pair apparatus is observed in some cilia and flagella (Omoto and Kung, 1980; Omoto and Witman, 1981; Kamiya, 1982; Hosokawa and Miki-Noumura, 1987; Omoto et al., 1999), and has also been suggested for the sea urchin sperm flagella (Gibbons et al., 1987; Shingyoji et al., 1991b; Takahashi et al., 1991). Since in the sea urchin sperm and many other flagella and cilia, the plane including the central pair is perpendicular to the plane of beat, it is thought that as the central pair rotates, a signal regulating the activity of dynein is transmitted from the central pair to the dynein arms via the radial spokes.

Presumably, the regulatory signal from the central pair apparatus is mediated by the radial spokes (Smith and Sale, 1992) and modifies the dynein arm activity (Habermacher and Sale, 1995). This hypothesis receives support from the fact that the motility of paralyzed mutant flagella of *Chlamydomonas* that lack the central pair and radial spokes can be restored by an extragenic suppressor mutation that by-passes the need for the missing structures through a compensating alteration in one of the motor subunits of the dynein arms (Huang et al., 1982; Brokaw and Luck, 1985). In the present study, I found that the asymmetric bending pattern of flagella beating under imposed head vibration rotates around the flagellar axis when the vibrating plane is rotated, regardless of the concentration of Ca^{2+} but only under high ATP conditions. This seems to suggest that, at least at ATP

concentrations higher than ~100 μM, Ca^{2+} modifies the regulatory signal from the central pair, which is mediated by the radial spokes and controls the activity of the dynein arms. This idea is supported by the fact that the wild type *Chlamydomonas* flagella require the central pair for the Ca^{2+}-dependent conversion of their waveform at 1 mM ATP (Hosokawa and Miki-Noumura, 1987).

It is interesting that certain other properties of dynein, as well as the rotation of the bending pattern in the sea urchin sperm flagella, depend on whether the ATP concentration is above or below approximately 100 μM (Tanaka and Miki-Noumura, 1988; Shingyoji et al., 1995; Omoto et al., 1996; Yoshimura and Shingyoji, 1999). It is possible that different mechanisms regulate the activity of dynein in the two ATP concentration regimes. The Ca^{2+}-dependent regulation of dynein activity may also be closely related to these ATP-dependent mechanisms. As stated above, at higher ATP concentrations (≥100 μM), the central pair/radial spoke system seems to be essential for the Ca^{2+}-regulation of dynein activity in both sea urchin and *Chlamydomonas* flagella. In contrast, at lower ATP concentrations, it is shown that the central pair/radial spokes is not essential for the Ca^{2+}-dependent waveform conversion in *Chlamydomonas* (Wakabayashi et al., 1997). This seems to be consistent with our present result that at 27 μM MgATP (~50 μM ATP) I could observe Ca^{2+}-induced decrease in sliding velocity but not rotation of the bending pattern. The

mechanism by which Ca^{2+} regulates the dynein arm activity at lower ATP condition is not clear. However, since the ATP concentration in live sperm flagella is thought to be 5-10 mM (Gibbons and Gibbons, 1972), the central pair are likely to play an essential role in the Ca^{2+}-dependent regulation of dynein arm activity *in vivo*.

It was interesting that only the sliding responsible for the formation of the reverse bend was affected by Ca^{2+}. It is possible that the two singlet microtubules of the central pair are functionally asymmetrical in such a way that only one of them transmits the regulatory signal to the dynein through the radial spokes to regulate the sliding responsible for the formation of the reverse bend. Structural and biochemical differences between the two microtubules of the central pair have been shown in *Chlamydomonas* flagella (Mitchell and Sale, 1999).

Calmodulin has been known to be a component of sea urchin sperm axonemes (Burgess et al., 1980; Brokaw and Nagayama, 1985). It has been suggested to be responsible for increasing the asymmetry of the flagellar waveform in the presence of Ca^{2+} above 10^{-5} M in sea urchin sperm (Brokaw and Nagayama, 1985; Brokaw, 1991a). The present study has shown that TFP does not affect the Ca^{2+}-induced decrease of sliding velocity at 10^{-6}-10^{-5} M Ca^{2+} but inhibits the 'quiescence' at 10^{-4} M Ca^{2+}, restoring asymmetric flagellar beating with both the sliding velocity and the reverse bend angle similar to those obtained at 10^{-5} M Ca^{2+}. These results imply that in sea

urchin sperm flagella Ca^{2+}-calmodulin is not involved in the decrease of the microtubule sliding velocity induced by 10^{-6}-10^{-5} M Ca^{2+} but is involved in the regulation of sliding that leads to 'quiescence' at 10^{-4} M Ca^{2+}.

Calmodulin has been found in other flagella and cilia (Gitelman and Witman, 1980; Walter and Shultz, 1981), but its role has been unclear. In *Paramecium* cilia, the effect of TFP on the ciliary reversal caused by about 10^{-6} M Ca^{2+} are controversial: an inhibitory effect has been reported by Otter et al. (1984) whereas no such effect has been observed by Nakaoka et al. (1984). The difference may be due to different conditions of demembranation and reactivation since TFP can inhibit the ciliary reversal in the presence of cAMP (Izumi and Nakaoka, 1987). This indicates a possible involvement of protein phosphorylation in the regulation of dynein activity by Ca^{2+}-calmodulin. The localization of calmodulin within the axoneme is unknown, although immunoelectron microscopy of *Tetrahymena* cilia suggests that calmodulin localizes along the longitudinal axis of the doublet microtubules at regular intervals of about 90 nm (Ohnishi et al., 1982). Ohnishi et al. (1982) suggested the interdoublet links as possible calmodulin-binding sites. Some group of the inner dynein arms may also be a candidate for the calmodulin-binding sites, because their periodicity is close to the periodicity of the radial spokes (~96 nm) (Goodenough and Heuser, 1985). In *Chlamydomonas* flagella, the activity of the inner arm dynein is regulated by phosphorylation of a 138-kDa inner arm dynein intermediate chain

(Habermacher and Sale, 1995, 1997). Protein phosphorylation is also known to be involved in the regulation of flagellar movement in sea urchin sperm; 'quiescence' can be induced by phosphatase treatment, although the target protein of phosphorylation has not been identified (Takahashi et al., 1985). Thus, it is tempting to speculate that Ca^{2+}-calmodulin regulates the activity of dynein through protein phosphorylation.

The asymmetry and 'quiescence' of the sea urchin sperm flagella are known to be abolished by mild trypsin treatment (Brokaw and Simonick, 1977; Gibbons and Gibbons, 1980). In the present study, a similar treatment removed the Ca^{2+}-induced decrease of sliding velocity and 'quiescence'. This result indicates that the proteins responsible for these Ca^{2+}-induced responses are possibly digested by trypsin treatment. I will describe about the axonemal proteins affected by mild trypsin treatment in Part 2.

Taken together, the previous studies and the present results strongly indicate that Ca^{2+} decreases the microtubule sliding velocity by regulating the activity of dynein through the central pair apparatus and its associated structures at ATP concentrations higher than ~100 μM. Selective regulation of the activity of a group of dynein arms by Ca^{2+} would be a basis for the changes of the bending pattern of flagella brought about by a high Ca^{2+} concentration. I speculate that some of the trypsin-sensitive polypeptides, which may be components of the central pair, regulate microtubule sliding in a Ca^{2+} concentration-dependent manner. This will be discussed in Part 2.

Table 1. Effects of trifluoperazine (TFP) on microtubule sliding velocity and bend angle

Ca^{2+} (M)	TFP (μM)	Sliding velocity (rad/s)	Bend angle (rad)		n
			Principal bend	Reverse bend	
$<10^{-9}$	0	173.6±10.1	2.56±0.27	2.40±0.07	8
	25	181.2±16.0	2.79±0.30	2.39±0.33	4
	50	179.1±12.8	2.84±0.11	2.28±0.32	5
10^{-5}	0	151.7±27.6	2.67±0.60	1.67±0.23	5
	50	154.7±17.8	3.10±0.40	1.32±0.14	5
10^{-4}	0	[Quiescence]	[4.76±0.42]	—	6
	10	138.1±16.4	2.42±0.40	1.52±0.41	11

These data were obtained from the flagella vibrated at 35 Hz (250 μM MgATP). Values show mean ± s.d. Sliding velocities and bend angles were determined for 5-9 μm in the middle region about 15-25 μm from the base (in this region the propagating waves maintained their bend angle).

Fig. 1-1.

The device for vibrating the sperm head. The vibration frequency and amplitude are regulated by regulating frequency and voltage applied to piezoelectric bimorphs. (a) piezoelectric driver, (b) glass micropipette, (C) stage of inverted microscope

Fig. 1-1.

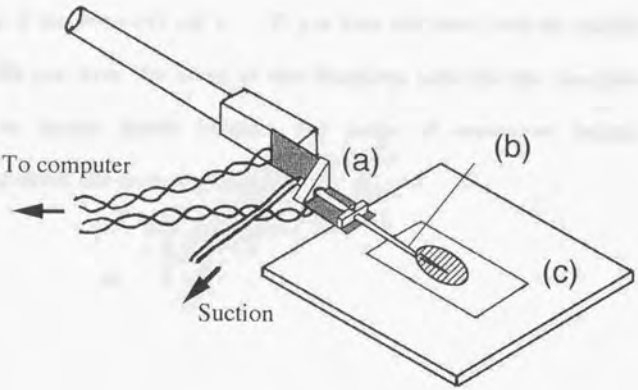

Fig. 1-2.

Typical tracings from video records of reactivated flagella vibrated at 26 Hz, 35 Hz, and 45 Hz. Demembranated spermatozoa were reactivated at 250 μM MgATP, in the absence ($<10^{-9}$ M) and in the presence (10^{-5} M) of Ca^{2+}. The head of the spermatozoa was held by a glass micropipette by suction and vibrated laterally. Prox. and Mid. indicate approximate position respectively of the proximal region (5-17 μm from the base) and the middle region (20-25 μm from the base) of the flagellum used for the analysis. Numbers by sperm heads indicate the order of successive images representing about one cycle of vibration.

Fig. 1-2.

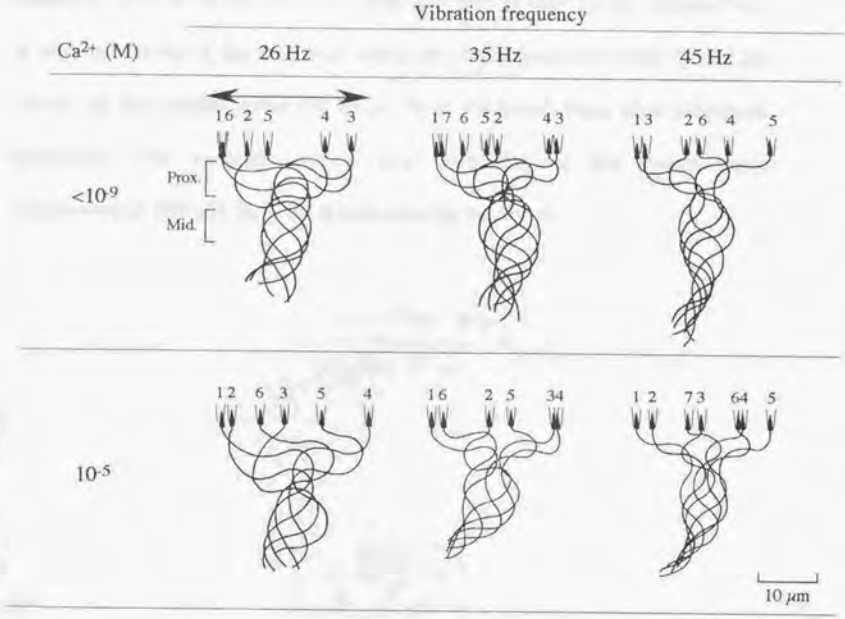
Vibration frequency
Ca2+ (M)
26 Hz
35 Hz
45 Hz
<10-9
Prox.
Mid.
16 2 5 4 3
17 6 52 43
13 26 4 5
10-5
12 6 3 5 4
16 2 5 34
12 73 64 5
10 μm

Fig. 1-3.

Effects of Ca^{2+} on the microtubule sliding velocity in reactivated flagella under imposed head vibration. Open and filled circles indicate the average values at $<10^{-9}$ M (sperm number, n=3) and 10^{-5} M Ca^{2+} (n=5), respectively. A, sliding velocity in the proximal region (5-17 μm from the base); B, sliding velocity in the middle region (20-25 μm from the base). Bars show standard deviations. The average natural beat frequency of the spermatozoa reactivated at 250 μM MgATP is indicated by an arrow.

Fig. 1-3.

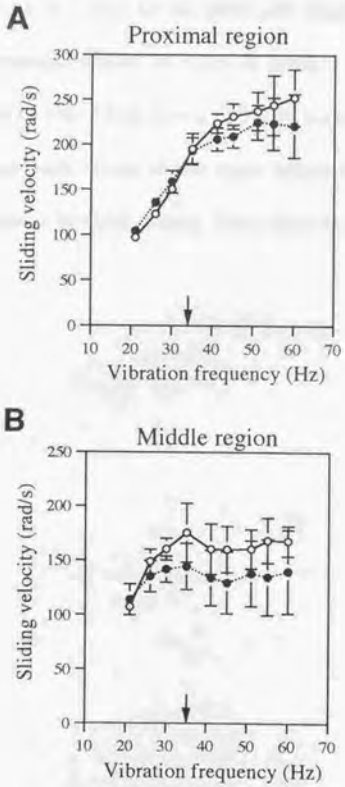
A
Proximal region
Sliding velocity (rad/s)
300
250
200
150
100
50
0
10 20 30 40 50 60 70
Vibration frequency (Hz)
B
Middle region
Sliding velocity (rad/s)
250
200
150
100
50
0
10 20 30 40 50 60 70
Vibration frequency (Hz)

Fig. 1-4.

Effects of Ca^{2+} on the microtubule sliding velocity (A), the reverse bend angle (B) and the principal bend angle (C) in the middle region under imposed vibration at 21 Hz, 35 Hz, and 45 Hz (250 μM MgATP). Open and filled boxes indicate the average values at $<10^{-9}$ M (n=6) and 10^{-5} M (n=7) Ca^{2+}, respectively. Values of the filled boxes (10^{-5} M Ca^{2+}) with asterisks are significantly different from those of the open boxes ($<10^{-9}$ M Ca^{2+}) at the same vibration frequency ($p<0.02$, t-test). Bars show standard deviations.

Fig. 1-4.

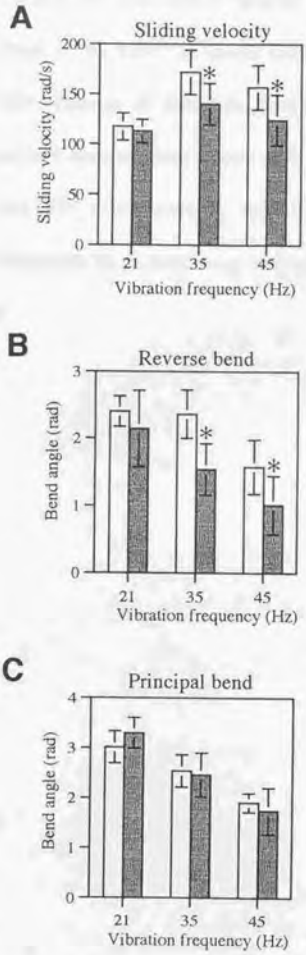
A
Sliding velocity
Sliding velocity (rad/s)
200
150
100
50
0
21
35
45
Vibration frequency (Hz)
B
Reverse bend
Bend angle (rad)
3
2
1
0
21
35
45
Vibration frequency (Hz)
C
Principal bend
Bend angle (rad)
4
3
2
1
0
21
35
45
Vibration frequency (Hz)

Fig. 1-5.

Effects of MgATP concentration on the maximal microtubule sliding velocity (A), the reverse bend angle (B) and the principal bend angle (C) in the middle region of the flagella at $<10^{-9}$ M (open circles) and 10^{-5} M (filled circles) Ca^{2+}. respectively. Values of the open circles ($<10^{-9}$ M Ca^{2+}) with asterisks are significantly different from those of the filled circles (10^{-5} M Ca^{2+}) at the same MgATP concentration ($p<0.02$, t-test). Bars show standard deviations. Numbers in parentheses indicate the numbers of the spermatozoa examined.

Fig. 1-5.

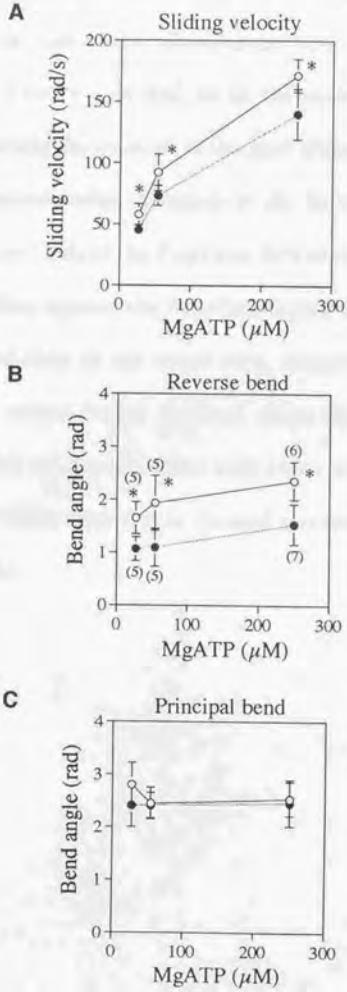
A
Sliding velocity
Sliding velocity (rad/s)
MgATP (μM)
B
Reverse bend
Bend angle (rad)
MgATP (μM)
C
Principal bend
Bend angle (rad)
MgATP (μM)

Fig. 1-6.

A, Schematic diagram showing the rotation of the beating plane. Imaginary planes are drawn at the back of the vibrating pipettes. These planes are parallel to the plane of beating as well as to the plane of vibration. B, Schematic diagram showing the rotation of the beat plane without rotation of peripheral doublet microtubules (Shingyoji et al., 1991b). A polystyrene bead attached to the lower side of the flagellum (left of the upper diagram) did not change its position against the flagellum during the rotation of the beat plane (middle and right of the upper row), suggesting that doublet microtubules does not rotate during the beat plane rotation. The lower diagram shows a possible mechanism of the beat plane rotation which may accompany the rotation of the central pair. Central pair may rotate with the rotation of the beat plane.

Fig. 1-6.

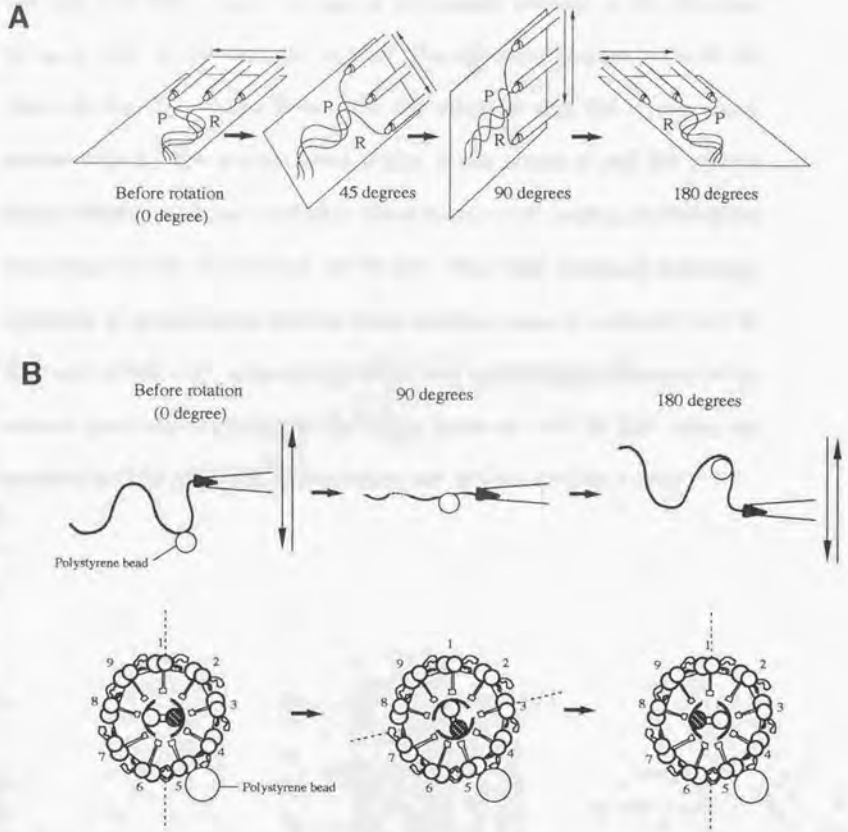
A
P
R
Before rotation
(0 degree)
45 degrees
90 degrees
180 degrees
B
Before rotation
(0 degree)
90 degrees
180 degrees
Polystyrene bead
Polystyrene bead

Fig. 1-7.

A, Typical waveforms of beating flagella for one cycle of beating, before (left tracings) and after (right tracings) a 180-degree rotation of the vibration plane at $<10^{-9}$ M Ca^{2+} and 10^{-5} M Ca^{2+}. The vibration frequency was 35 Hz (250 μM MgATP). P and R indicate the principal and the reverse bend, respectively. B, The average bend angles of the principal and the reverse bends before (open boxes) and after (filled boxes) a 180-degree rotation of the beat plane at $<10^{-9}$ M Ca^{2+} and 10^{-5} M Ca^{2+}. Bars show standard deviations. Numbers of spermatozoa used for these analyses were, 3 and 4 at $<10^{-9}$ M Ca^{2+} and 10^{-5} M Ca^{2+}, respectively. There was a significant difference in the reverse bend angles at 10^{-5} M Ca^{2+} from those at $<10^{-9}$ M Ca^{2+} after the rotation ($p<0.02$, t-test) as well as before the rotation ($p<0.05$, t-test).

Fig. 1-7.

A

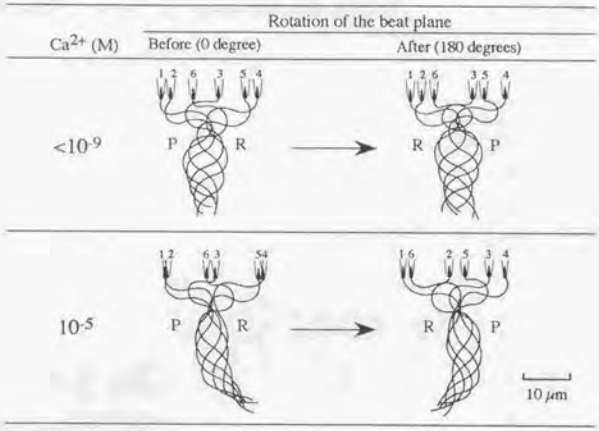
Rotation of the beat plane
Ca2+ (M)
Before (0 degree)
After (180 degrees)
<10-9
10-5
1 2 6 3 5 4
P
R
1 2 6 3 5 4
R
P
1 2 6 3 5 4
P
R
1 6 2 5 3 4
R
P
10 μm

B

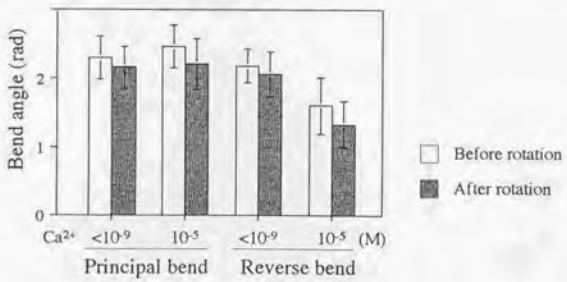
Bend angle (rad)
0
1
2
Ca2+ <10-9 10-5 <10-9 10-5 (M)
Principal bend
Reverse bend
Before rotation
After rotation

Fig. 1-8.

Typical tracings of the trypsin-treated flagella. Demembranated spermatozoa were reactivated at 250 μM MgATP, in the absence ($<10^{-9}$ M) and in the presence (10^{-6} M) of Ca^{2+} and vibrated at 35 Hz.

Fig. 1-8.

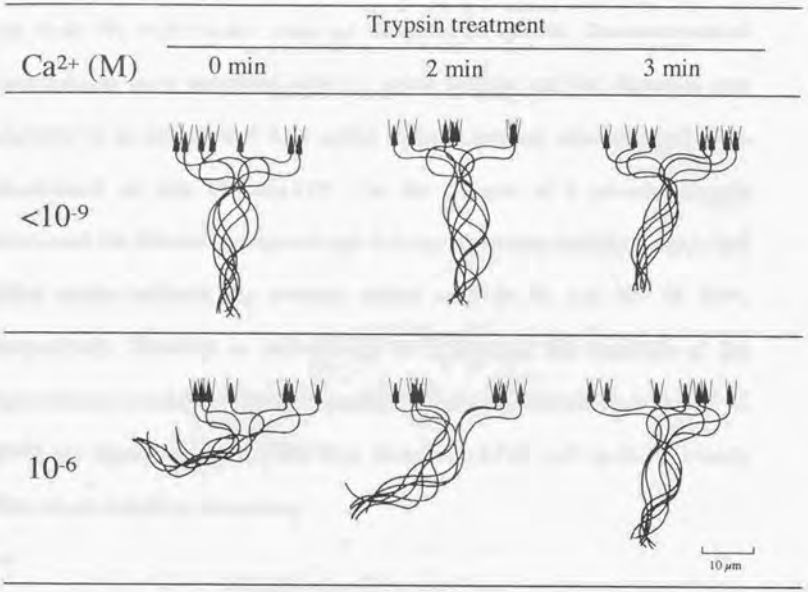

Fig. 1-9.

Effects of trypsin treatment on microtubule sliding velocity (A), the reverse bend angle (B) and the principal bend angle (C) in the middle region (10-20 μm from the base) under imposed vibration at 35 Hz. Demembranated spermatozoa were incubated with 0.1 μg/ml trypsin and the digestion was stopped by an addition of 0.25 μg/ml soybean trypsin inhibitor, and then reactivated at 250 μM MgATP. For the sample of 0 minute trypsin treatment the solution contained only 0.25 μg/ml trypsin inhibitor. Open and filled circles indicate the average values at $<10^{-9}$ M and 10^{-6} M Ca^{2+}, respectively. Numbers in parentheses in B indicate the numbers of the spermatozoa examined for each condition. Values with asterisks ($<10^{-9}$ M Ca^{2+}) are significantly different from those at 10^{-6} M Ca^{2+} ($p<0.02$, t-test). Bars show standard deviations.

Fig. 1-9.

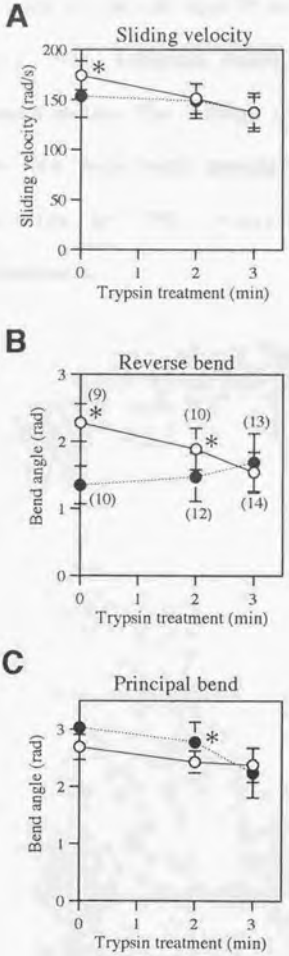
A
Sliding velocity
Sliding velocity (rad/s)
200
150
100
50
0
0
1
2
3
Trypsin treatment (min)
B
Reverse bend
Bend angle (rad)
3
2
1
0
(9)
(10)
(13)
(10)
(12)
(14)
0
1
2
3
Trypsin treatment (min)
C
Principal bend
Bend angle (rad)
3
2
1
0
0
1
2
3
Trypsin treatment (min)

Fig. 1-10.

Effects of trifluoperazine (TFP) and mild trypsin treatment on the waveform of sperm flagella reactivated at 250 μM MgATP in the presence of 10^{-4} M Ca^{2+}. Almost 100% sperm were quiescent before treatment. After each treatment, flagella became motile. The tracings of beating flagella were obtained for the sperm with their heads attached to the glass surface. *Hemicentrotus pulcherrimus* for TFP treatment and *Anthocidaris crassispina* for trypsin treatment.

Fig. 1-10.

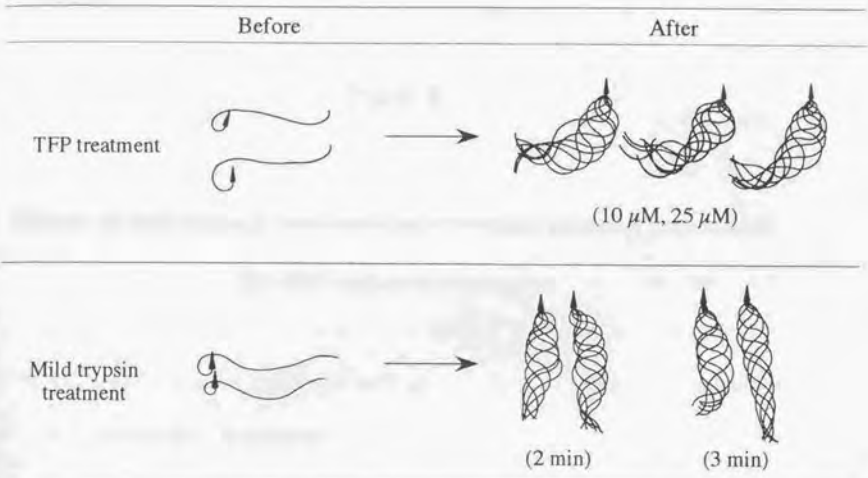
Before
After
TFP treatment
(10 μM, 25 μM)
Mild trypsin treatment
(2 min)
(3 min)

Part 2

Effects of mild trypsin treatment on axonemal proteins responsible for Ca^{2+}-induced responses

SUMMARY

The asymmetry and 'quiescence' of the sea urchin sperm flagella induced by a high concentration of Ca^{2+} was abolished by mild trypsin treatment (Part 1). To identify the axonemal components involved in these calcium-induced responses, I studied the effect of mild trypsin treatment on the axonemal proteins. Demembranated flagella of the sea urchin, *Hemicentrotus pulcherrimus* and *Anthocidaris crassispina*, were treated with 0.1 μg/ml trypsin for 2 or 3 minutes and reactivated at 0.5 mM ATP. These flagella showed more symmetric waveforms than those of untreated flagella at 10^{-6} M Ca^{2+}. The Ca^{2+}-induced asymmetry at 10^{-6} M Ca^{2+} was abolished partially by a 2-minute trypsin treatment and completely by a 3-minute treatment. The induction of quiescence at 10^{-4} M Ca^{2+} was completely inhibited by a mild trypsin treatment longer than 2 minutes. The study using SDS-polyacrylamide gel electrophoresis revealed that at least twelve polypeptides were digested from these trypsin treated axonemes. Of the twelve, eleven seemed to be digested by a 2-minute trypsin treatment and calmodulin was one of them. This is consistent with the result that the 2-minute trypsin treatment restored beating of quiescent flagella at 10^{-4} M Ca^{2+} as well as the calmodulin antagonists. The remaining (~160 kDa) polypeptide was probably digested only by a 3-minute treatment. Thus, it seems possible that the ~160 kDa polypeptide might be associated with the Ca^{2+}-induced asymmetry and the Ca^{2+}-induced decrease of sliding velocity.

INTRODUCTION

An increase of the intracellular concentration of Ca^{2+} modifies the waveform of eukaryotic cilia and flagella (Naitoh and Kaneko, 1972; Holwill and McGregor, 1976; Hyams and Borisy, 1978; Brokaw, 1979, 1991). In Part 1, I showed that the microtubule sliding velocity in reactivated sea urchin sperm flagella beating under imposed head vibration decreases with an increase in the Ca^{2+} concentration up to 10^{-6}-10^{-5} M. In the previous studies, in which velocity of sliding disintegration was measured in the trypsin-treated axonemes, the effect of Ca^{2+} was not observed (Walter and Satir, 1979; Mogami and Takahashi, 1983; Okagaki and Kamiya, 1986). These results suggest that the axonemal proteins important for the Ca^{2+}-induced decrease in the sliding velocity are damaged by trypsin treatment.

In the sliding disintegration experiments, ≥2 μg/ml trypsin was used. Such trypsin treatment does not abolish the sliding activity of dynein (Summers and Gibbons, 1971), but disrupts axonemal structures such as radial spokes and nexin links (Summers and Gibbons, 1973). Moreover, the axonemes treated with trypsin lost the ability of cyclical bending (Shingyoji and Takahashi, 1995b). These results imply that some of the trypsin-sensitive proteins may be quite important for regulation of axonemal beating as well as for Ca^{2+} responses.

When the axonemes are mildly treated with 0.1 μg/ml trypsin in the presence of ATP, the axonemes beat for several minutes before they

disintegrate even at high Ca^{2+} concentration. During this treatment, asymmetrical beating and quiescence induced by high Ca^{2+} are gradually abolished (Brokaw and Simonick, 1977; Gibbons and Gibbons, 1980; and also the results in Part. 1). In Part 1, I showed that The Ca^{2+}-induced decrease in the sliding velocity was removed by the 3-minute mild trypsin treatment while the quiescence was inhibited by the treatment longer than 2 minutes. These results indicate that the mild-trypsin treatment may digest some protein responsible for the Ca^{2+}-induced decrease in the sliding velocity and quiescence. In Part 2, I analysed the effects of mild trypsin treatment on the axonemal components in order to speculate possible axonemal polypeptides associated with the Ca^{2+} responses.

Ca^{2+}-binding proteins may be associated with the Ca^{2+}-responses. Among Ca^{2+}-binding proteins, calmodulin has been well studied in many cilia and flagella. Calmodulin exists in sea urchin sperm flagella (Brokaw and Nagayama, 1985) and suggested to be involved in a Ca^{2+}-induced increase in asymmetry (Brokaw and Nagayama, 1985; Brokaw, 1991a). However, definite role and localization of calmodulin in sea urchin sperm flagella is remain to be elucidated. In this study, I also focued on the role of calmodulin in the Ca^{2+} responses.

In Part 2, I examined the effects of the mild trypsin treatment on the axonemal proteins and obtained the preliminary results showing that twelve polypeptides involving calmodulin were affected by trypsin. Among

the twelve polypeptides, ~160 kDa polypeptide, which was probably digested at a 3-minute mild trypsin treatment seems to be related to asymmetrical beating and the Ca^{2+}-induced decrease of the sliding velocity at 10^{-6} M Ca^{2+}. On the other hand, calmodulin, which was mostly digested by a 2-minute treatment may be associated with the induction of quiescence at 10^{-4} M Ca^{2+}.

MATERIALS AND METHODS

Demembranation and mild trypsin treatment

Spermatozoa of the sea urchin, *Hemicentrotus pulcherrimus* and *Anthocidaris crassispina*, were diluted with Ca^{2+}-free artificial sea water containing 465 mM NaCl, 10 mM KCl, 25 mM $MgSO_4$, 0.2 mM ethylenediaminetetraacetic acid (EDTA) and 2 mM Tris-HCl (pH 8.2) to give an optical density reading of 0.2 when diluted with 1:100 with artificial sea water. Diluted spermatozoa were demembranated with 6 volumes of demembranating solution. Demembranation was carried out under potentially asymmetric conditions (Gibbons and Gibbons, 1980), and the demembranating solution contained 0.04% (w/v) CHAPS (3-[(3-cholamidopropyl) dimethylammonio]-1-propane-sulphonate), 0.01% (w/v) Nonidet P-40, 0.2 M potassium acetate, 2 mM $MgSO_4$, 2 mM glycoletherdiamine-N, N, N', N'-tetraacetic acid (EGTA), 20 mM Tris-HCl (pH 8.2), and 1 mM dithiothreitol (DTT). After 45 seconds, the extracted

sperm suspension was added to 11 volumes of reactivating solution (0.2 M potassium acetate, 2 mM $MgSO_4$, 2 mM EGTA, 20 mM Tris-HCl (pH 8.2), and 1 mM DTT) and containing 0.1 μg/ml trypsin (SIGMA, Type III) (Brokaw and Simonick, 1977). Digestion was carried out for 2 and 3 minutes at 27.0 ±0.1°C and was stopped with an addition of an excess volume (0.25 μg/ml for motility and 10 μg/ml for SDS-PAGE) of soybean trypsin inhibitor (SIGMA, Type I-S). For motility observation, 2 μl of trypsin-treated spermatozoa were reactivated in 1 ml of reactivating solution containing 2% (w/v) polyethylene glycol (Mr 20×10^3) and 250 μM MgATP with or without 10^{-6}-10^{-4} M Ca^{2+}.

SDS-polyacrylamide gel electrophoresis (SDS-PAGE)

Axonemal samples for SDS-PAGE were obtained as follows: demembranated and trypsin-treated axonemes were homogenized and sperm heads were separated from the fragmented axonemes by centrifugation (Yoshimura and Shingyoji, 1999). SDS-PAGE was done with standard methods (Laemmli, 1970) by using 4% and 12% polyacrylamide gels. Gels were stained with Coomassie blue or silver. The amount of proteins loaded on the 4% gels and 12% gels which were stained with Coomassie blue were 100 μg/lane and 60 μg/lane, respectively. In a 4% gel stained with silver, 6.4 μg portion of each sample were electrophoresed. For observation of the mobility shift of calmodulin, 12% gel and running buffer, both containing either 0.1 mM EGTA or 0.1 mM $CaCl_2$ (Burgess et al., 1980)

were used. Density of bands on the SDS-PAGE was analysed by using a computer with NIH image software ver. 1.62.

RESULTS

Effects of mild trypsin treatment on the Ca^{2+}-induced changes of flagellar waveforms

Fig. 2-1 shows typical tracings of beating flagella treated with mild trypsin for 2-3 minutes at $<10^{-9}$ M, 10^{-6} M and 10^{-4} M Ca^{2+}. At 10^{-6} M Ca^{2+}, untreated flagella showed asymmetrical beating. After treatment with mild trypsin for 2 minutes, the waveform was still asymmetrical but more symmetrical than those of the untreated axonemes. After a 3-minute treatment, the flagella beat symmetrically at 10^{-6} M Ca^{2+} as those at $<10^{-9}$ M. These changes in asymmetry were similar to those observed in the flagella during head vibration shown in Part 1 (Fig. 1-8 in Part 1).

At 10^{-4} M Ca^{2+}, untreated flagella showed quiescence. Mild trypsin treatment over 2 minutes removed the quiescence and resumed flagellar beating (Fig. 2-1). The beating of flagella was symmetrical both in 2-minute and 3-minute treated axonemes. These changes in the flagellar waveforms by mild trypsin treatment were observed in both *Hemicentrotus* and *Anthocidaris*.

Effects of mild trypsin treatment on axonemal components

Fig. 2-2 shows the effect of mild trypsin treatment for 2 and 3 minutes on the polypeptide bands of the axonemes analysed by 4% (Fig. 2-2A, right) SDS-polyacrylamide gel electrophoresis (SDS-PAGE) stained with Coomassie Blue, and their densitometry patterns (Fig. 2-2A, left). Dynein heavy chains were apparently unaffected by the trypsin-treatment. However, among the other bands, at least eleven bands in 4% gel appeared to be affected by the trypsin treatment. Of the eleven bands, two larger polypeptides (approximately 830 and 700 kDa; indicated with diamonds in Fig. 2-2A) were completely digested, and eight polypeptides (approximately 310, 290, 280, 230, 215, 195, 150 and 140 kDa; indicated with single asterisks in Fig. 2-2A) were reduced in the 2 minutes-treated axonemes. The eight bands in the 4% gel showed only a slight or no further reduction by subsequent treatment with trypsin for another minute (the 3 minutes-treated axonemes: single asterisks in the densitometry patterns in Fig. 2-2 A). In the 3 minutes-treated axonemes, only one band of ~160 kDa (indicated with a double-asterisk in Fig. 2-2A) was largely affected. I also examined the amount of this ~160 kDa polypeptide with silver staining and found that ~160 kDa polypeptide was completely digested in 3 minutes-treated axonemes (indicated with a double-asterisk in Fig. 2-2B).

I confirmed these changes of axonemal polypeptides induced by mild trypsin treatment in four separate experiments by using three 4% gels

stained with Coomassie Blue and a 4% gel stained with silver. I obtained basically similar results in the four gels but with slight differences in band appearances in 2 minutes-treated axonemes. The amount of ~160 kDa polypeptide also varied among four gels; ~160 kDa polypeptide was almost unaffected by a 2-minute treatment in three gels (including Fig. 2-2A), while it was partially digested in one gel (Fig. 2-2B). On the other hand, complete digestion of the ~160 kDa band by a 3-minute treatment was observed in all gels. For more precise information, however, I should use a two-dimensional electrophoresis.

I further examined the effects of mild trypsin treatment on the smaller polypeptides than ~100 kDa by using 12% gel. I found that two bands (21.5 and 17.9 kDa, indicated with single asterisks in Fig. 2-3A) were affected in the 2 minutes-treated axonemes. Similar decrease of the amount of these two polypeptide bands was observed in three separate experiments. The 21.5 kDa and 17.9 kDa bands were likely to be calmodulin because their molecular weights are similar to those representing two Ca^{2+} binding states of calmodulin. The mobility of calmodulin changes when the Ca^{2+} concentration is changed in the sample buffer (Brokaw and Nagayama, 1985; Gitelman and Witman, 1980) or in the SDS-polyacrylamide gels (Burgess et al., 1980). I examined the effects of Ca^{2+} on these two bands in the axonemes by using 12% SDS-polyacrylamide gel and running buffer, which contain 0.1 mM EGTA or 0.1 mM $CaCl_2$. SDS-PAGE analysis using

untreated axonemes revealed that only the 21.5 kDa band was observed in the presence of 0.1 mM EGTA (Fig. 2-3B, left) while only the 17.9 kDa band was observed in the presence of 0.1 mM $CaCl_2$ (Fig. 2-3B, right). Similar results were obtained when EGTA and $CaCl_2$ were applied on the sample buffer instead of the gel. These sizes of the bands with and without Ca^{2+} are close to those of calmodulin previously reported in sea urchin sperm flagella and *Chlamydomonas* (Brokaw and Nagayama, 1985; Burgess et al., 1980; Gitelman and Witman, 1980). Thus, I conclude that the two bands in the 12% gel (Fig. 2-3A) probably represent the two states of calmodulin.

DISCUSSION

In Part 2, I found that twelve polypeptides, containing calmodulin, were digested by a mild trypsin treatment. Among the twelve, only a ~160 kDa polypeptide seemed to be completely digested by a 3-minute trypsin treatment while it seemed to remain almost intact in 2 minutes-treated axonemes. A similar 3-minute treatment removed the Ca^{2+}-induced decrease in the sliding velocity and the quiescence, while the quiescence was also abolished by a 2-minute treatment. Therefore, the presence or absence of the ~160 kDa polypeptide seems to be closely associated with the changes in the waveform asymmetry (Fig. 2-1) and the decrease in the sliding velocity (Part 1, Fig. 1-9). Thus, it is possible that the ~160 kDa polypeptide might be associated with the decrease in sliding velocity observed at 10^{-6} M

Ca^{2+}. At the present time, however, the possibility of contribution of other polypeptides that were affected by the 2 minute-treatment cannot be excluded.

Interestingly, four of the twelve polypeptides that were digested either partially or completely by the mild trypsin treatment had molecular weights (700, 280, 160 and 140 kDa) close to those (630, 265, 165 and 142 kDa) of some components of the central pair apparatus of *Chlamydomonas* flagella (Dutcher, et al., 1984; Mitchell and Sale, 1999). The sizes of the components of the radial spokes (22-123 kDa), however, were different from the sizes of any of the twelve polypeptides (Piperno et al., 1981). It is tempting to speculate that the ~160 kDa polypeptide, together with some of the other ten polypeptides that were digested by the mild trypsin treatment might be components of the central pair apparatus.

The main results of Part 1 and Part 2 are summarized in Fig. 2-4. In these studies, I found that the microtubule sliding velocity in beating sea urchin sperm flagella decreases at 10^{-6} M Ca^{2+} and that this Ca^{2+}-induced decrease in sliding velocity may be regulated through the central pair at least at ATP concentrations higher than ~100 μM. Furthermore, I found that both the Ca^{2+}-induced waveform changes and the Ca^{2+}-induced decrease in sliding velocity were inhibited partially by a 2-minute mild trypsin treatment and abolished completely by a 3-minute treatment, while the quiescence induced

by 10^{-4} M Ca^{2+} was inhibited by a 2-minute trypsin treatment. These results indicate that the mechanism responsible for quiescence at 10^{-4} M Ca^{2+} are different from that responsible for the decrease in sliding velocity observed at 10^{-6} M Ca^{2+}. The effects of the 2-minute mild trypsin treatment on the flagellar waveform and on the sliding velocity were similar to those of calmodulin antagonists TFP and W-7. These results suggest that calmodulin is important for the induction of quiescence but not for the decrease in the microtubule sliding velocity. The result in Part 2, showing that the mild trypsin treatment for longer than 2 minutes digested calmodulin and inhibited the quiescence, supports this idea. As I have discussed above, some of the trypsin sensitive polypeptides (involving the ~160 kDa) may be associated with the regulation of the Ca^{2+}-induced decrease in sliding velocity and play a different role from that of calmodulin in the Ca^{2+} responses.

In the present study, I showed for the first time that the microtubule sliding velocity is regulated by Ca^{2+} concentration through the central pair at high ATP conditions. The mechanism regulating the dynein activity by some signal from the central pair to provide the decrease in sliding velocity, however, remains unclear. This will be the next question we have to investigate.

Fig. 2-1.

Typical tracings from video records of flagella of *Anthocidaris* spermatozoa beating with their head attached to the slideglass. Spermatozoa treated with 0.1 μg/ml trypsin for 2 or 3 minutes were reactivated at 250 μM MgATP, in the absence ($<10^{-9}$ M) and in the presence (10^{-6} and 10^{-4} M) of Ca^{2+}. The tracings at 10^{-4} M Ca^{2+} were the same tracings as used in Fig. 1-10.

Fig. 2-1.

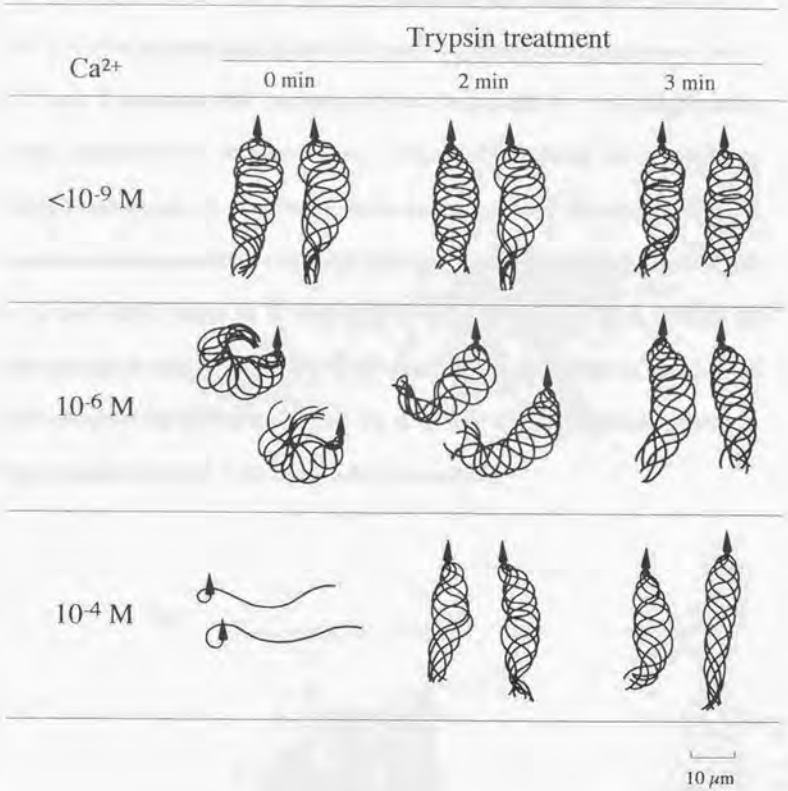

Fig. 2-2.

SDS-PAGE analysis of trypsin treated axonemes of *Hemicentrotus* spermatozoa using 4% SDS-polyacrylamide gels. A, Coomassie Blue-stained gels (right) and their densitometry patterns of the bands corresponding to 140-310 kDa polypeptides (left) after mild trypsin (0.1 μg/ml) treatment for 0, 2 and 3 minutes. DHC indicates dynein heavy chains. Two polypeptides bands indicated by diamonds were completely digested by a 2-minute trypsin treatment. B, a part of silver-stained gels of the trypsin-treated axonemes corresponding to 140-200 kDa polypeptides. At least eight bands in A and three bands in B indicated by single asterisks were reduced in amount by the trypsin treatment for 2 minutes. A polypeptide of about ~160 kDa indicated by a double asterisk (in A and B) completely disappeared in the axonemes treated with trypsin for 3 minutes.

Fig. 2-2.

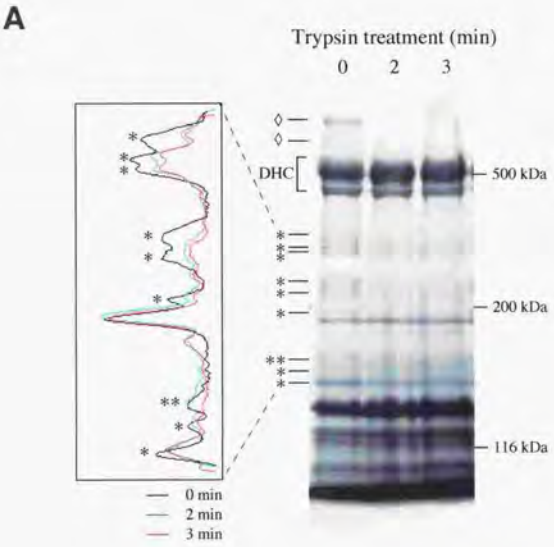
A
Trypsin treatment (min)
0 2 3
DHC
500 kDa
200 kDa
116 kDa
0 min
2 min
3 min
B
Trypsin treatment (min)
0 2 3
200 kDa

Fig. 2-3.

A, Coomassie Blue stained 12% SDS-polyacrylamide gels of trypsin-treated axonemes of *Hemicentrotus* spermatozoa (right) and their densitometry patterns of the bands (left) corresponding to 17-23 kDa polypeptides. Two bands of 17.9 kDa and 21.5 kDa indicated by asterisks were affected by trypsin treatment. B, Ca^{2+} dependent mobility shift of two bands of 21.5 kDa and 17.9 kDa affected by trypsin. The axonemal proteins of *Anthocidaris* spermatozoa were electrophoresed in the presence of either 0.1 mM EGTA or 0.1 mM $CaCl_2$ in 12% gels. 21.5 kDa band appeared in the gel containing 0.1 mM EGTA shifted to 17.9 kDa band in the gel containing 0.1 mM $CaCl_2$.

Fig. 2-3.

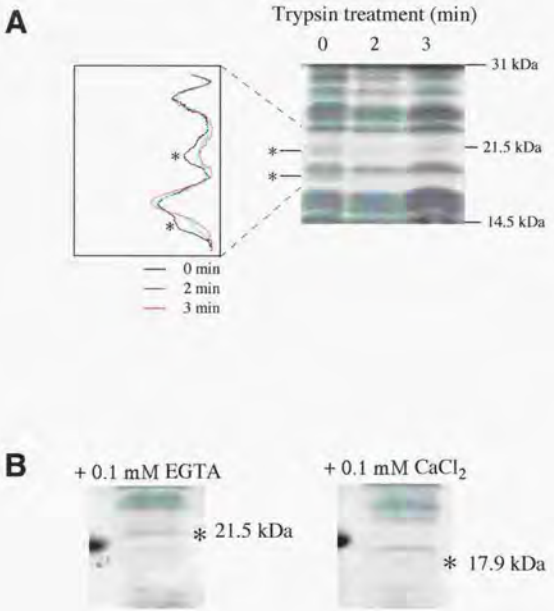
A
Trypsin treatment (min)
0
2
3
31 kDa
21.5 kDa
14.5 kDa
*
*
*
0 min
2 min
3 min
B
+ 0.1 mM EGTA
* 21.5 kDa
+ 0.1 mM CaCl2
* 17.9 kDa

Fig. 2-4.

Schematic diagram showing the main results obtained in Part 1 and Part 2. Beating flagella increase their waveform asymmetry at 10^{-7}-10^{-5} M Ca^{2+} and become quiescent at 10^{-4} M Ca^{2+}. The microtubule sliding velocity within beating flagella is decreased by an increase of Ca^{2+}. This decrease in sliding velocity is mediated by the central pair apparatus at ATP concentrations higher than ~100 μM. A mild trypsin treatment for 2 and 3 minutes abolishes the quiescence and the Ca^{2+}-induced decrease in sliding velocity (Part 1), respectively. And the calmodulin antagonists (TFP and W-7) also inhibits the quiescence (Part 1). Among the polypeptides affected by a mild trypsin treatment, only a ~160 kDa polypeptide was digested by a 3-minute treatment, while calmodulin was digested by a 2-minute treatment (Part 2). These results suggest that the ~160 kDa polypeptide and calmodulin may be associated with the Ca^{2+}-induced decrease in sliding velocity and the quiescence, respectively.

Fig. 2-4.

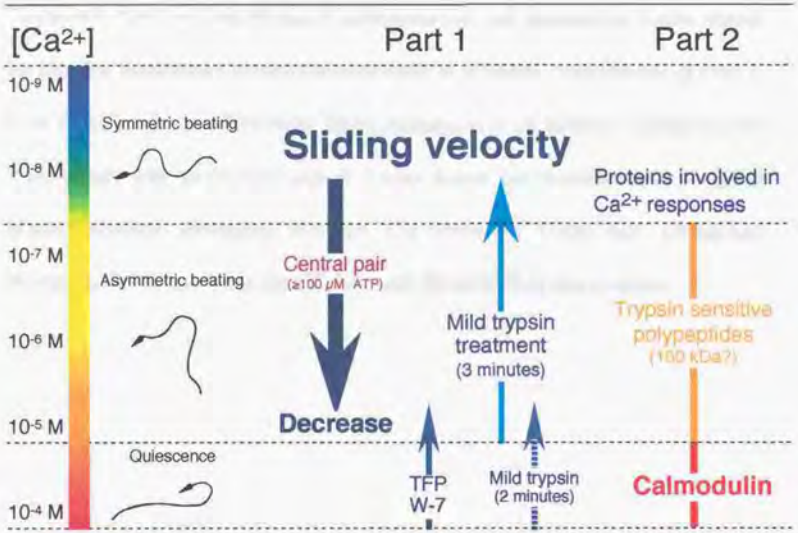
[Ca2+]
Part 1
Part 2
10-9 M
10-8 M
10-7 M
10-6 M
10-5 M
10-4 M
Symmetric beating
Asymmetric beating
Quiescence
Sliding velocity
Central pair
(≥100 μM ATP)
Decrease
Mild trypsin
treatment
(3 minutes)
TFP
W-7
Mild trypsin
(2 minutes)
Proteins involved in
Ca2+ responses
Trypsin sensitive
polypeptides
(100 kDa?)
Calmodulin

Acknowledgement

I would like to express my sincere gratitude to my thesis adviser, Dr Chikako Shingyoji, for her thoughtful guidance, kind advice and encouragement throughout this study. I would be also thankful to Professor Keiichi Takahashi for his kind advice, encouragement and discussion. I also thank Dr Misako Yoshimura for her collaboration in rotation experiments of Part 1. I am also thankful to Professor Ritsu Kamiya and Dr Kenjiro Yoshimura for their advice and technical support. I also thank the directors and staffs of Misaki Marine Biological Station, University of Tokyo and Ushimado Marine Laboratory, Okayama University, for providing sea urchins.

References

Bessen, M., Fay, R. B. and Witman, G. B. (1980). Calcium control of waveform in isolated flagellar axonemes of *Chlamydomonas*. *J. Cell Biol.* 86, 446-455.

Brokaw, C. J. and Gibbons, I. R. (1975). Mechanisms of movement in flagella and cilia. *In Swimming and Flying in Nature*. (Ed. Wu, T. Y-T., Brokaw, C. J. and Brennen C.), pp. 89-126. New York: Plenum Publishing Corp.

Brokaw, C. J. and Simonick, T. F. (1977). Motility of Triton-demembranated sea urchin sperm flagella during digestion by trypsin. *J. Cell Biol.* 75, 650-665.

Brokaw, C. J. (1979). Calcium-induced asymmetrical beating of Triton-demembranated sea urchin sperm flagella. *J. Cell. Biol.* 82, 401-411.

Brokaw, C. J. and Luck, D. J. L. (1985). Bending patterns of *Chlamydomonas* flagella: III. A radial spoke head deficient mutant and a central pair deficient mutant. *Cell Motil.* 5, 195-208.

Brokaw, C. J. and Nagayama, S. M. (1985). Modulation of the asymmetry of sea urchin sperm flagellar bending by calmodulin. *J. Cell Biol.* 100, 1875-1883.

Brokaw C. J. (1989). Direct measurements of sliding between outer doublet microtubules in swimming sperm flagella. *Science* 243, 1593-1596.

Brokaw, C. J. (1991a). Calcium sensors in sea urchin sperm flagella. *Cell Motil. Cytoskel.* 18, 123-130.

Brokaw, C. J. (1991b). Microtubule sliding in swimming sperm flagella: direct and indirect measurements on sea urchin and tunicate spermatozoa. *J. Cell Biol.* 114, 1201-1215.

Burgess, W. H., Jemiolo, D. K. and Kretsinger, R. H. (1980). Interaction of calcium and calmodulin in the presence of sodium dodecyl sulfate. *Biochim. Biophys. Acta* 623, 257-270.

Dutcher, S. K., Huang, B. and Luck, D. J. L. (1984). Genetic dissection of the central pair microtubules of the flagella of *Chlamydomonas reinhardtii*. *J. Cell Biol.* 98, 229-236.

Eshel, D. and Gibbons, I. R. (1989). External mechanical control of the timing of bend initiation in sea urchin sperm flagella. *Cell Motil. Cytoskel.* 14, 416-423.

Fox, L. A. and Sale, W. S. (1987). Direction of force generation by the inner row of dynein arms on flagellar microtubules. *J. Cell Biol.* 105, 1781-1787.

Gee, M. A., Heuser, J. E. and Vallee, R. B. (1997). An extended microtubule-binding structure within the dynein motor domain. *Nature* 390, 636-639.

Gibbons, B. H. and Gibbons, I. R. (1972). Flagellar movement and adenosine triphosphatase activity in sea urchin sperm extracted with

Triton X-100. *J. Cell Biol.* 54, 75-97.

Gibbons, B. H. (1980). Intermittent swimming in live sea urchin sperm. *J. Cell. Biol.* 84, 1-12.

Gibbons, B. H. and Gibbons, I. R. (1980). Calcium-induced quiescence in reactivated sea urchin sperm. *J. Cell Biol.* 84, 13-27.

Gibbons, I. R. (1963). Studies on the protein components of cilia from *Tetrahymena Pyriformis*. *Proc. Natl. Acad. Sci. USA* 50, 1002-1010.

Gibbons, I. R. and Rowe, A. J. (1965). Dynein: a protein with adenosine triphosphate activity from cilia. *Science* 149, 424-426.

Gibbons, I. R., Shingyoji, C., Murakami, A. and Takahashi, K. (1987). Spontaneous recovery after experimental manipulation of the plane of beat in sperm flagella. *Nature* 325, 351-352.

Gitelman, S. E. and Witman, G. B. (1980). Purification of calmodulin from *Chlamydomonas*: calmodulin occurs in cell bodies and flagella. *J. Cell Biol.* 98, 764-770.

Goodenough, U. W. and Heuser, J. E. (1982). Substructure of the outer dynein arm. *J. Cell Biol.* 95, 798-815.

Goodenough, U. W and Heuser, J. E. (1984). Structural comparison of purified dynein proteins with *in situ* dynein arms. *J. Mol. Biol.* 180, 1083-1118.

Goodenough, U. W. and Heuser, J. E. (1985). Substructure of inner dynein arms, radial spokes, and the central pair/projection complex of

cilia and flagella. *J. Cell Biol.* 100, 2008-2018.

Habermacher, G. and Sale, W. S. (1995). Regulation of dynein-driven microtubule sliding by an axonemal kinase and phosphatase in *Chlamydomonas* flagella. *Cell Motil. Cytoskel.* 32, 106-109.

Habermacher, G. and Sale, W. S. (1997). Regulation of flagellar dynein by phosphorylation of a 138-kD inner arm dynein intermediate chain. *J. Cell Biol.* 136, 167-176.

Holwill, M. E. J. and McGregor, J. L. (1976). Effects of calcium on flagellar movement in the trypanosome *Crithidia oncopelti*. *J. Exp. Biol.* 65, 229-242.

Hosokawa, Y. and Miki-Noumura, T. (1987). Bending motion of *Chlamydomonas* axonemes after extrusion of central-pair microtubules. *J. Cell Biol.* 105, 1297-1301.

Huang, B., Ramanis, Z. and Luck, D. J. L. (1982). Suppressor mutations in *Chlamydomonas* reveal a regulatory mechanism for flagellar function. *Cell* 28, 115-124.

Hyams, J. S. and Borisy, G. G. (1978). Isolated flagellar apparatus of *Chlamydomonas*: characterization of forward swimming and alteration of waveform and reversal of motion by calcium ions *in vitro*. J. Cell Sci. 33, 235-253.

Izumi, A. and Nakaoka, Y. (1987). cAMP-mediated inhibitory effect of calmodulin antagonists on ciliary reversal of *Paramecium*. *Cell Motil.*

Cytoskel. 7, 154-159.

Johnson, K. A. (1983). The pathway of ATP hydrolysis by dynein. Kinetics of a presteady state phosphate burst. *J. Biol. Chem.* 258, 13825-13832.

Kagami, O. and Kamiya, R. (1992). Translocation and rotation of microtubules caused by multiple species of *Chlamydomonas* inner-arm dynein. *J. Cell Sci.* 103, 653-664.

Kamiya, R. (1982). Extrusion and rotation of the central-pair microtubules in detergent-treated *Chlamydomonas* flagella. *Cell Motil. Suppl.* 1, 169-173.

Katada, J., Shingyoji, C. and Takahashi, K. (1989). Effects of detergents used to demembranate the sea-urchin spermatozoa on the reactivated flagellar movement, with special reference to the rotatability of the plane of flagellar beat. *Cell Struct. Funct.* 14, 751-758.

Laemmli, U. K. (1970). Cleavage of structural proteins during the assembly of the head of bacteriophage T4. *Nature* 227, 680-685.

Mitchell, D. R. and Sale, W. S. (1999). Characterization of a *Chlamydomonas* insertional mutant that disrupts flagellar central pair microtubule-associated structures. *J. Cell Biol.* 144, 293-304.

Mogami, Y. and Takahashi, K. (1983). Calcium and microtubule sliding in ciliary axonemes isolated from *Paramecium caudatum*. *J. Cell. Sci.* 61, 107-121.

Naitoh, Y. and Kaneko, H. (1972). Reactivated Triton-extracted models of *Paramecium*: modification of ciliary movement by calcium ions. *Science* 176, 523-524.

Nakaoka, Y., Tanaka, H. and Oosawa, F. (1984). Ca^{2+}-dependent regulation of beat frequency of cilia in *Paramecium*. *J. Cell Sci.* 65, 223-231.

Ohnishi, K., Suzuki, Y. and Watanabe, Y. (1982). Studies on calmodulin isolated from *Tetrahymena* cilia and its localization within the cilium. *Exp. Cell Res.* 137, 217-227.

Okagaki, T. and Kamiya, R. (1986). Microtubule sliding in mutant *Chlamydomonas* axonemes devoid of outer or inner dynein arms. *J. Cell. Biol.* 103, 1895-1902.

Omoto, C. K. and Kung, C. (1980). Rotation and twist of the central-pair microtubules in the cilia of *Paramecium*. *J. Cell. Biol.* 87, 33-46.

Omoto, C. K. and Witman, G. B. (1981). Functionally significant central-pair rotation in a primitive eukaryotic flagellum. *Nature* 290, 708-710.

Omoto, C. K. and Johnson, K. A. (1986). Activation of dynein adenosinetriphosphate by microtubules. *Biochemistry* 25, 419-427.

Omoto, C. K. (1991). Mechanochemical coupling in cilia. *Int. Rev. Cytol.* 131, 255-292.

Omoto, C. K., Yagi, T., Kurimoto, E. and Kamiya, R. (1996). Ability of paralyzed flagella mutants of *Chlamydomonas* to move. *Cell Motil. Cytoskel.* 33, 88-94.

Omoto, C. K., Gibbons, I. R., Kamiya, R., Shingyoji, C., Takahashi, K. and Witman, G. B. (1999). Rotation of the central pair microtubules in eukaryotic flagella. *Mol. Biol. Cell* 10, 1-4.

Otter, T., Satir, B. H. and Satir, P. (1984). Trifluoperazine-induced changes in swimming behavior of paramecium: evidence for two sites of drug action. *Cell Motil.* 4, 249-267.

Piperno, G., Huang, B., Ramanis, Z. and Luck, D. J. L. (1981). Radial spokes of *Chlamydomonas* flagella: polypeptide composition and phosphorylation of stalk components. *J. Cell Biol.* 88, 73-79.

Porter, M. E. and Johnson K. A. (1989). Dynein structure and function. *Annu. Rev. Cell Biol.* 5, 119-151.

Rüffer, U. and Nultsch, W. (1991). Flagellar photoresponses of Chlamydomonas cells held on micropipettes: II. Changes in flagellar beat pattern. *Cell Motil. Cytoskel.* 18, 269-278.

Sakakibara, H. and Nakayama, H. (1998). Translocation of microtubules caused by the αβ, β and γ outer arm dynein subparticles of *Chlamydomonas*. *J. Cell. Sci.* 111, 1155-1164.

Sale, W. S. and Satir, P. (1977). Direction of active sliding of microtubules in *Tetrahymena* cilia. *Proc. Natl. Acad. Sci. USA* 74, 2045-

2049.

Sale, W. S., Goodenough, U. W. and Heuser, J. E. (1985). The substructure of isolated and in situ outer dynein arms of sea urchin sperm flagella. *J. Cell Biol.* 101, 1400-1412.

Sale, W. S. (1986). The axonemal axis and Ca^{2+}-induced asymmetry of active microtubule sliding in sea urchin sperm tails. *J. Cell Biol.* 102, 2042-2052.

Sale, W. S. and Fox, L. A. (1988). Isolated β-heavy chain subunit of dynein translocates microtubules *in vitro*. *J. Cell Biol.* 107, 1793-1797.

Satir, P. and Sale, W. S. (1977). Tails of *Tetrahymena*. *J. Protozool.* 24, 498-501.

Satir, P. (1982). Mechanisms and controls of microtubule sliding in cilia. In *Symp. Soc. Exp. Biol.* Vol. 35, *Prokaryotic and Eukaryotic Flagella* (ed. Amos, W. B. and Duckett, J. G.), pp. 179-201. Cambridge: Cambridge University Press.

Satir, P. (1985). Switching mechanism in the control of ciliary motility. *Modern Cell Biol.* 4, 1-46.

Schmidt, J. A. and Eckert, R. (1976). Calcium couples flagellar reversal to photostimulation in *Chlamydomonas reinharditii*. *Nature* 262, 713-715.

Shingyoji, C., Murakami, A., Takahashi, K. (1977). Local reactivation of Triton-extracted flagella by iontophoretic application of ATP. *Nature,*

265, 269-270.

Shingyoji, C., Gibbons, I. R., Murakami, A. and Takahashi, K. (1991a). Effect of imposed head vibration on the stability and waveform of flagellar beating in sea urchin spermatozoa. *J. Exp. Biol.* 156, 63-80.

Shingyoji, C., Katada, J., Takahashi, K. and Gibbons, I. R. (1991b). Rotating the plane of imposed vibration can rotate the plane of flagellar beating in sea-urchin sperm without twisting the axoneme. *J. Cell. Sci.* 98, 175-181.

Shingyoji, C. and Takahashi, K. (1995a). Flagellar quiescence responce in sea urchin sperm induced by electric stimulation. *Cell Motil. Cytoskel.* 31, 59-65.

Shingyoji, C. and Takahashi, K. (1995b). Cyclical bending movements induced locally by successive iontophoretic application of ATP to an elastase-treated flagellar axoneme. *J. Cell. Sci.* 108, 1359-1369.

Shingyoji, C., Yoshimura, K., Eshel, D., Takahashi, K. and Gibbons, I. R. (1995). Effect of beat frequency on the velocity of microtubule sliding in reactivated sea urchin sperm flagella under imposed head vibration. *J. Exp. Biol.* 198, 645-653.

Smith, E. F. and Sale, W. S. (1992). Regulation of dynein-driven microtubule sliding by the radial spokes in flagella. *Science* 257, 1557-1559.

Summers K. E. and Gibbons, I. R. (1971). Adenosine triphosphate-induced sliding of tubules in trypsin-treated flagella of sea-urchin sperm flagella. *Proc. Natl. Acad. Sci. USA* 68, 3092-3096.

Summers K. E. and Gibbons, I. R. (1973). Effects of trypsin digestion on flagellar structures and their relationship to motility. *J. Cell Biol.* 58, 618-629.

Takahashi, D., Murofushi, H., Ishiguro, K., Ikeda, J. and Sakai, H. (1985). Phosphoprotein phosphatase inhibits flagellar movement of Triton models of sea urchin spermatozoa. *Cell Struct. Funct.* 10, 327-337.

Takahashi, K., Shingyoji, C. and Kamimura, S. (1982). Microtubule sliding in reactivated flagella. In *Symp. Soc. exp. Biol.* Vol.35, *Prokaryotic and Eukaryotic Flagella* (ed. Amos, W. B. and Duckett, J. G.), pp.159-177. Cambridge: Cambridge University Press.

Takahashi, K., Shingyoji, C., Katada, J., Eshel, D. and Gibbons, I. R. (1991). Polarity in spontaneous unwinding after prior rotation of the flagellar beat plane in sea-urchin spermatozoa. *J. Cell Sci.* 98, 183-189.

Tamm, S. L. and Tamm, S. (1981). Ciliary reversal without rotation of axonemal structures in ctenophore comb plates. *J. Cell Biol.* 89, 495-509.

Tamm, S. L. and Tamm, S. (1984). Alternate patterns of doublet microtubule sliding in ATP-disintegrated macrocilia of the ctenophore *Beroë*. *J. Cell Biol.* 99 (pt1), 1364-1371.

Tanaka, M. and Miki-Noumura, T. (1988). Stepwise sliding disintegration of *Tetrahymena* ciliary axonemes at higher concentrations of ATP. *Cell Motil. Cytoskel.* 9, 191-204.

Tani, T. and Kamimura, S. (1999). Dynein-ADP as a force-generating intermediate revealed by a rapid reactivation of flagellar axoneme. *Biophys. J.* 77, 1518-1527.

Tsukita, S., Tsukita, S., Usukura, J. and Ishikawa, H. (1983). ATP-dependent Structural changes of the outer dynein arm in *Tetrahymena* cilia: a freeze-etch replica study. *J. Cell Biol.* 96, 1480-1485.

Vale, R. D. and Toyoshima, Y. Y. (1989). Microtubule translocation properties of intact and proteolytically digested dyneins from *Tetrahymena* cilia. *J. Cell Biol.* 108, 2327-2334.

Wais-Steider, J. and Satir, P. (1979). Effect of vanadate on gill cilia: switching mechanism in ciliary beat. *J. Supramol. Struct.* 11, 339-347.

Wakabayashi, K., Yagi, T. and Kamiya, R. (1997). Ca^{2+}-dependent waveform conversion in the flagellar axoneme of Chlamydomonas mutants lacking the central-pair/radial spoke system. *Cell Motil. Cytoskel.* 38, 22-28.

Walter, M. F. and Satir, P. (1979). Calcium does not inhibit active sliding of microtubules from mussel gill cilia. *Nature* 278, 69-70.

Walter, M. F. and Schultz, J. E. (1981). Calcium receptor protein calmodulin isolated from cilia and cells of *Paramecium tetraurelia*. *Eur.*

J. Cell Biol. 24, 97-100.

Yano, Y. and Miki-Noumura, T. (1980). Sliding velocity between outer doublet microtubules of sea-urchin sperm axonemes. *J. Cell Sci.* 44, 169-186.

Yoshimura, M. and Shingyoji, C. (1999). Effects of the central pair apparatus on microtubule sliding velocity in sea urchin sperm flagella. *Cell Struct. Funct.* 24, 43-54.

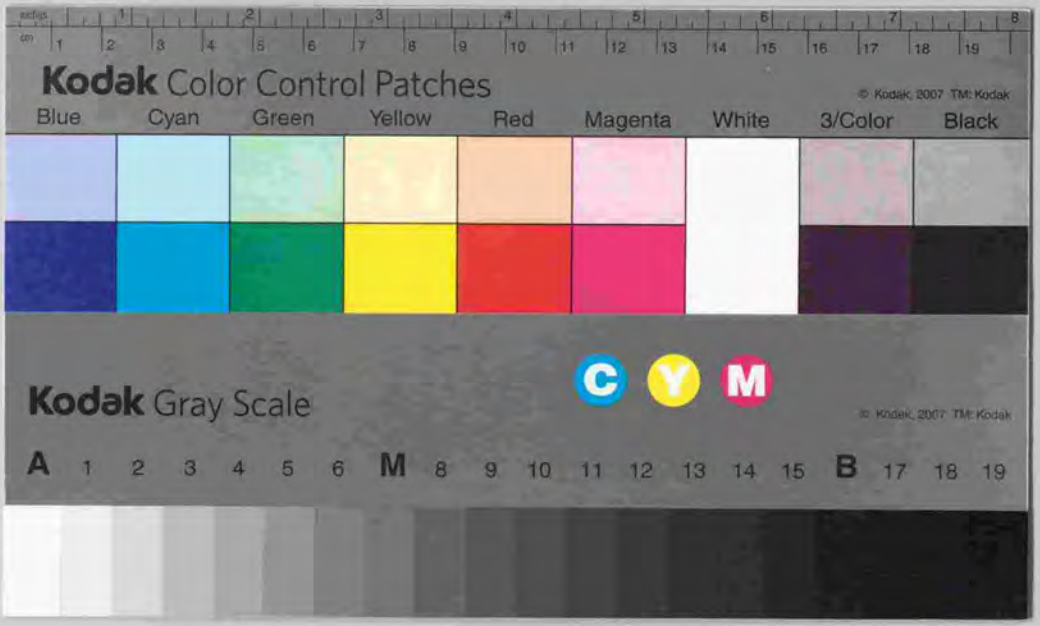
Kodak Color Control Patches
© Kodak, 2007 TM: Kodak
Blue
Cyan
Green
Yellow
Red
Magenta
White
3/Color
Black
Kodak Gray Scale
C
Y
M
© Kodak, 2007 TM: Kodak
A 1 2 3 4 5 6 M 8 9 10 11 12 13 14 15 B 17 18 19